Sound & Vibration 2026, 60(2), 3949.
doi: https://doi.org/10.59400/sv3949

Article

A hybrid fuzzy–probabilistic methodology for machinery reliability assessment via vibration testing

Yogeesh N.[1,2,*], Asokan Vasudevan[3], Mohammed Almakki[4], Puspanathan Doraisingam[3], Khan Sarfaraz Ali[3]

[1] Research Fellow, INTI International University, Nilai 71800, Malaysia
[2] Department of Mathematics, Government First Grade College, Tumakuru 572102, India
[3] Faculty of Business and Communications, INTI International University, Nilai 71800, Malaysia
[4] School of Engineering, Architecture and Interior Design, Amity University Dubai, Dubai 345019, United Arab Emirates
*** Corresponding author:** Yogeesh N., yogeesh.r@gmail.com

CITATION

N. Y, Vasudevan A, Almakki M, et al. A hybrid fuzzy–probabilistic methodology for machinery reliability assessment via vibration testing. Sound & Vibration. 2026; 60(2): 3949. https://doi.org/10.59400/sv3949

ARTICLE INFO

Received: 23 January 2026
Revised: 21 February 2026
Accepted: 12 March 2026
Available online: 22 April 2026

Abstract: Vibration-based condition monitoring is widely used to infer machinery reliability, but practical decisions are often undermined by two coupled uncertainty sources: (i) stochastic variability in measured vibration features and (ii) epistemic ambiguity in thresholds, feature–damage mappings, and prior assumptions. This study proposes a hybrid fuzzy–probabilistic reliability framework that preserves probabilistic meaning for time-to-failure while explicitly propagating imprecision arising in vibration interpretation. Time–frequency and time-domain vibration features are first normalized and fused into a monotone health severity index using a transparent fuzzy inference layer. Reliability is then modelled through a Weibull/proportional-hazards (PH) formulation, and uncertain quantities (failure thresholds, mapping parameters, priors) are represented by fuzzy numbers. Using α-cut decomposition of this study, the fuzzy parameter set is vibrated/propagated through the PH hazard and cumulative hazard to obtain interval-valued survival/reliability curves and failure-risk bounds with respect to time, together with RUL quantiles for planning. A confidence factor of this study derived from feature variability gates hazard inflation so that risk increases only when evidence is both severe and trustworthy. Here on an experimental vibration dataset express that the adopted method yields interpretable reliability envelopes, supports conservative maintenance decisions through lower-bound reliability, and provides validation outputs aligned with time-to-event prediction.

Keywords: hybrid uncertainty; machinery reliability; fuzzy inference systems; proportional hazards model; Weibull time-to-failure; α-cut propagation; interval reliability bounds; remaining useful life (RUL)

1. Introduction

1.1. Background: Machinery reliability and vibration testing

Machinery reliability assessment quantifies the probability that a component performs its intended function over time under specified operating conditions. Let $T \geq 0$ denote the time-to-failure random variable. The standard reliability descriptors are

$$R(t) = Pr(T > t),\ f(t) = \frac{d}{dt}(1 - R(t)),\ h(t) = \lim_{\Delta t \to 0^+} \frac{\Pr(t \leq T < t + \Delta t \mid T \geq t)}{\Delta t} = \frac{f(t)}{R(t)}.$$

Equivalently, the cumulative hazard $H(t) = \int_0^t h(\tau)d\tau$ yields

$$R(t) = \exp(-H(t)).$$

In vibration-based condition monitoring, the machine state is inferred from vibration measurements (e.g., accelerometer signals) by extracting feature vectors in time, frequency, or time-frequency domains (e.g., RMS, kurtosis, spectral band energies, resonance indicators). Practical measurement issues-sensor bandwidth, mounting stiffness, noise, operating variability (speed/load/temperature), and intermittent transients-introduce variability and bias in, which can propagate into reliability conclusions if not explicitly handled [1, 2]. Comprehensive reviews detail best practices for vibration measurement and analysis, including feature robustness under nonstationarity [3–7]. Complementary diagnostic studies use fuzzy reasoning and wavelet/frequency features for bearing and pump faults [8–10], and recent deep-learning approaches further motivate multi-domain feature sets [11–14].

A mathematically direct route from vibration evidence to reliability is covariate survival modeling, where vibration-derived covariates modulate the hazard. A common choice is a proportional hazards (PH) structure,

$$h(t \mid \phi) = h_0(t)\exp\left(\beta^\top z(t)\right)$$

where $h_0(t)$ is a baseline hazard and $z(t)$ is a normalized condition indicator derived from $\phi(t)$. Under this model,

$$R(t \mid \phi) = \exp\left(-\int_0^t h_0(\tau)\exp\left(\beta^\top z(\tau)\right)d\tau\right),$$

when a Weibull baseline is used,

$$h_0(t) = \frac{k}{\lambda}\left(\frac{t}{\lambda}\right)^{k-1},\ k > 0, \lambda > 0,$$

the model remains analytically interpretable and supports risk-based maintenance planning; prior vibration-monitoring studies show that condition indicators can modify hazard and thereby change replacement/maintenance policies [14–16]. Multi-channel monitoring extensions (e.g., combining vibration with other sensing streams) have also been shown to improve degradation representation within Weibull-type reliability formulations under realistic environments [17].

1.2. Motivation for a hybrid fuzzy–probabilistic methodology

As per this study, purely probabilistic survival model is well opted when uncertainty is dominated by randomness and sufficient failure data exist, however it becomes less transparent when key inputs-damage thresholds, degradation stages, feature-to-fault semantics-are basically imprecise. Conversely, a purely fuzzy scoring approach can express linguistic knowledge and ambiguity, but it does not naturally produce time-based reliability quantities such as $R(t), h(t)$, or RUL distributions needed for maintenance scheduling [18–20]. Related fuzzy vibration-control and

vibration optimization studies by the authors illustrate complementary fuzzy modeling capabilities that motivate the present uncertainty-aware reliability fusion [21–24].

To address this, we adopt a hybrid pipeline with three tightly coupled mathematical components:

(i) Probabilistic layer (time-to-failure reliability):
Map vibration covariates to hazard and reliability via survival modeling, e.g.,

$$h(t \mid z) = h_0(t)\exp\left(\beta^\top z(t)\right),\ R(t \mid z) = \exp\left(-\int_0^t h(\tau \mid z)d\tau\right)$$

where $h_0(t)$ may be Weibull and $z(t)$ is a condition indicator derived from vibration features [3,4,7].

(ii) Fuzzy layer (epistemic representation of vibration health):
Convert uncertain, linguistically described condition information into fuzzy health states.
Concretely, we define fuzzy sets for health categories (e.g., $\widetilde{S} \in \{$Normal, Degraded, Severe$\}$) through membership functions $\mu_{\widetilde{S}}(\phi)$, producing a fuzzy severity estimate and an associated uncertainty/confidence measure [5,6,9].

(iii) Fusion step (probability with explicit imprecision propagation):
Represent uncertain parameters as fuzzy numbers $\widetilde{\theta}$.
Using α-cut decomposition,

$$\widetilde{\theta} \Rightarrow \theta^{(\alpha)} = \left[\theta_L^{(\alpha)}, \theta_U^{(\alpha)}\right],\ \alpha \in [0,1],$$

we propagate parameter intervals through the survival model to obtain interval-valued hazards and reliability

$$h^{(\alpha)}(t) \in \left[h_L^{(\alpha)}(t), h_U^{(\alpha)}(t)\right],\ R^{(\alpha)}(t) \in \left[R_L^{(\alpha)}(t), R_U^{(\alpha)}(t)\right].$$

This yields reliability envelopes that remain statistically interpretable while transparently reflecting epistemic ambiguity. This hybrid structure is motivated by the need for decision-grade reliability from vibration testing, probabilistic where randomness dominates, fuzzy where knowledge is imprecise, and fused so that maintenance planning can be based on conservative bounds rather than overconfident point estimates.

1.3. Objectives of this study

This study focusses majorly on four objectives:

(1) Develop a mathematical modelling for vibration-to-reliability mapping using a covariate survival formulation.
(2) Design to study and know fuzzy inference system to represent epistemic uncertainty in vibration health states.
(3) Uses both layers to produce reliability metrics $R(t)$, hazard $h(t)$, and RUL intervals under uncertain testing conditions under this study.

(4) Demonstrate and evaluated the method using an experimental dataset to establish the results under this study using numerical output.

To know visually, **Figure 1** presents the end-to-end methodology as a two-layer uncertainty-aware pipeline. Here, vibration experiments provide acceleration responses $x(t)$ across operating regimes. These signals/vibrations are transformed into a feature vector $\phi(t)$ together with variability measures that summarize measurement and operating scatter. Then, it will survival/reliability block uses the covariates $z(t) = g(\phi(t))$ to parameterize the hazard $h(t \mid z)$ and reliability $R(t) = \exp\left(-\int_0^t h(\tau \mid z)d\tau\right)$. In this, along with a fuzzy inference block converts linguistically defined condition states into a severity score $s(t) \in [0, 1]$ and an evidence confidence $c(t) \in [0, 1]$ that shows epistemic ambiguity in thresholds and labels. Final outputs by adjusting the baseline hazard using (s, c), yielding an interval-aware reliability trajectory and decision quantities such as risk within a planning horizon, maintenance triggers, and an RUL band as per this study.

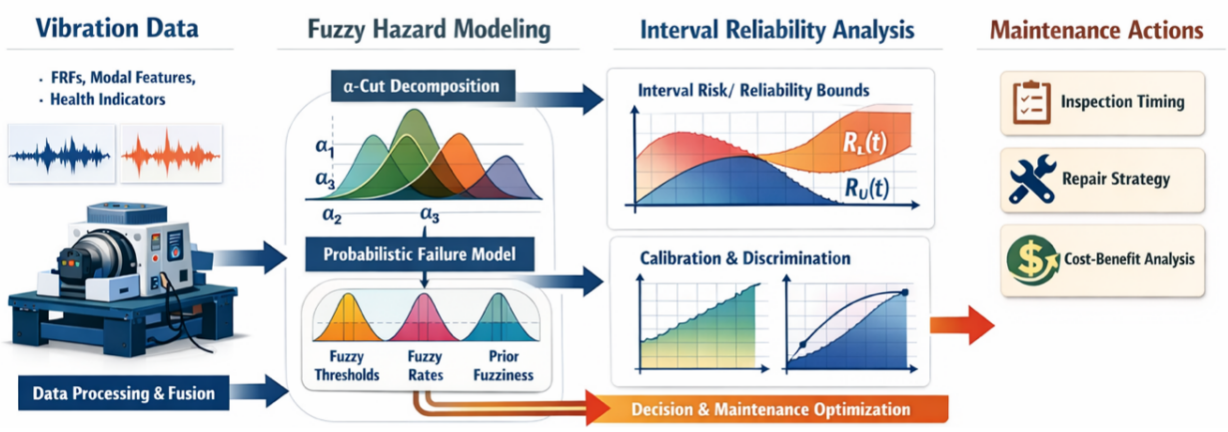

Figure 1. Conceptual architecture of the hybrid fuzzy-probabilistic reliability pipeline.

2. Preliminaries and notation

2.1. Vibration signal model and measurement notation

Let $x(t)$ represents the measured vibration signal over a finite record $t \in [0, T_0]$ along with sampling frequency f_s, we obtain samples

$$x[n] = x\left(\frac{n}{f_s}\right), \; n = 0, 1, \ldots, N-1, \; N = T_0 f_s.$$

A convenient decomposition is

$$x(t) = s(t; \theta) + \varepsilon(t),$$

where $s(t; \theta)$ is the (possibly non-stationary) vibration response governed by operating parameters θ (speed, load, temperature), and $\varepsilon(t)$ is measurement noise and unmodeled dynamics. Sensor bandwidth and mounting influence $\varepsilon(t)$ and feature bias/variance [2].

2.2. Time-to-failure, survival, and hazard (reliability theory)

Let T denote time to failure. Define:

$$F(t) = \Pr(T \le t),\ R(t) = 1 - F(t) = \Pr(T > t),$$

$$f(t) = \frac{d}{dt}F(t),\ h(t) = \frac{f(t)}{R(t)}.$$

For a Weibull baseline (used widely in machinery),

$$R_0(t) = \exp\left[-\left(\frac{t}{\eta}\right)^{\beta}\right],\ h_0(t) = \frac{\beta}{\eta}\left(\frac{t}{\eta}\right)^{\beta-1},$$

where $\beta > 0$ is the shape and $\eta > 0$ is the scale. Condition monitoring is incorporated by making hazard depend on vibration covariates, as in proportional hazards formulations used in vibration monitoring maintenance optimization [3,4].

2.3. Covariate representation from vibration features

At inspection/test instance k, define a feature vector

$$z_k = [z_{k1}, z_{k2}, \ldots, z_{kp}]^{\top} \in \mathrm{R}^p,$$

extracted from the vibration record. Typical features include RMS, kurtosis, crest factor, band energy, and envelope-spectrum peak amplitudes [1]. Under operational variability, z_k is random; we treat

$$z_k = \bar{z}_k + \delta z_k,$$

where $\bar{z}_k$ is the repeatable component (mean feature under controlled conditions) and δz_k captures variability and noise (estimated from repetitions). This is crucial because $h(t)$ should not be updated from a single noisy feature estimate [2,4].

2.4. Fuzzy sets for epistemic/linguistic uncertainty

A fuzzy set A on universe U is defined by a membership function $\mu_A : U \to [0,1]$ [5]. For vibration condition terms (e.g., "Low", "Medium", "High" RMS), we define membership functions $\mu_{\text{Low}}(z), \mu_{\text{Med}}(z),\ \mu_{\text{High}}(z)$. Fuzzy sets provide a mathematically consistent way to encode expert rules and incomplete threshold knowledge (epistemic uncertainty) [6,9].

2.5. Separation of uncertainty: Aleatory vs. epistemic

We explicitly distinguish:

- Aleatory uncertainty: randomness in T and z_k due to inherent variability → modeled probabilistically in survival/hazard updating [3,4].
- Epistemic uncertainty: ambiguity in state boundaries, expert assessments, model-form vagueness → handled by fuzzy sets and inference [5,6,9].

This below **Table 1** provide the mathematical symbols for vibration signals, features, reliability functions, and fuzzy variables used in this study.

Table 1. Notation used in this study.

Symbol	Meaning
$x(t), x[n]$	vibration signal (continuous/sampled)
f_s, N, T_0	sampling frequency, samples, record duration
z_k	feature vector extracted at instance k
T	time-to-failure random variable
$R(t), F(t), f(t)$	reliability, CDF, PDF
$h(t)$	hazard rate
β, η	Weibull shape and scale parameters
$\mu_A(\cdot)$	membership function of fuzzy set A
$H \in [0,1]$	fuzzy health index (defuzzified)

3. Vibration testing protocol and feature construction

3.1. Vibration signal model, acquisition, and preprocessing

Let $x(t)$ denote the measured acceleration signal from a sensor mounted on the machine housing. After sampling at rate $f_s(Hz)$, we obtain a discrete-time record

$$x[n] = x\left(nT_s\right),\ T_s = \frac{1}{f_s},\ n = 0, 1, \ldots, N-1.$$

To reduce bias from offsets and slow drifts, the record is detrended and normalized:

$$\widetilde{x}[n] = \frac{x[n] - \bar{x}}{\sigma_x},\ \bar{x} = \frac{1}{N}\sum_{n=0}^{N-1} x[n],\ \sigma_x^2 = \frac{1}{N-1}\sum_{n=0}^{N-1}(x[n] - \bar{x})^2.$$

Because vibration signals are commonly non-stationary under variable load/speed, the analysis is performed over K short frames (segments) of length L with overlap $\varrho \in [0, 1)$. For frame k, define

$$\widetilde{x}_k[n] = \widetilde{x}[n + k(1-\varrho)L],\ n = 0, \ldots, L-1,$$

and apply a window $w[n]$ (e.g., Hann) to control leakage:

$$y_k[n] = w[n]\widetilde{x}_k[n],\ \sum_{n=0}^{L-1} w^2[n] = 1.$$

This establishment enables both (i) feature extraction and (ii) explicit variability estimation across frames, which is essential when operating conditions fluctuate and measurement noise is non-negligible. Addition to that, any regime descriptors available during acquisition are stored as covariates

$$r_k = \left[\omega_k, L_{d,k}, \Theta_k, \ldots\right],$$

to support the regime-aware modeling and also avoid confounding "condition" with "operating mode" [1,2].

Figure 2 which is placed above is the experimental vibration-testing configuration used to generate the acceleration record $x(t)$ (sampled as $x[n]$ at

rate f_s). Accelerometers are positioned at fault-sensitive locations that defect-induced resonances are captured with adequate bandwidth, while controlled excitation is applied through a shaker. A required tachometer produces a phase reference to enable order-aware interpretation under varying speed.

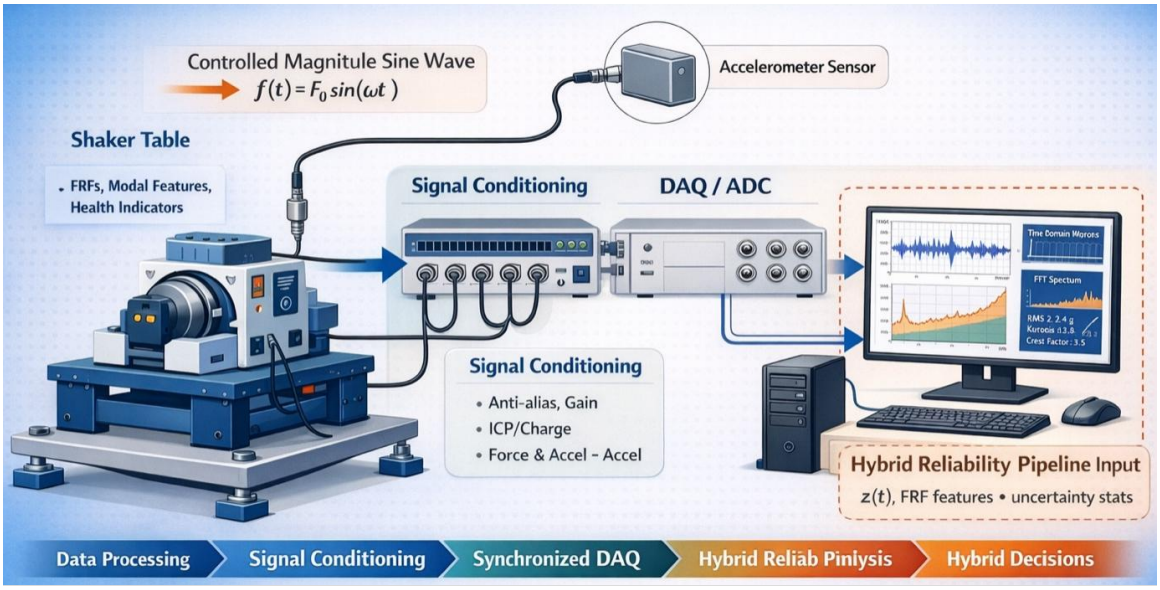

Figure 2. Schematic of vibration test configuration and data acquisition.

3.2. Multi-domain vibration feature extraction

For each frame k, we compute a feature vector $\phi_k \in \mathrm{R}^p$ using complementary time-, frequency-, and time-frequency-domain descriptors [1, 2]. Representative definitions (used as a template for the study's feature set) include:

3.2.1. Time-domain statistics

$$\mathrm{RMS}_k = \sqrt{\frac{1}{L}\sum_{n=0}^{L-1} y_k^2[n]},\ \mathrm{P2P}_k = \max_n y_k[n] - \min_n y_k[n],$$
$$\mathrm{Kurt}_k = \frac{\frac{1}{L}\sum_n (y_k[n]-\bar{y}_k)^4}{\left(\frac{1}{L}\sum_n (y_k[n]-\bar{y}_k)^2\right)^2},\ \mathrm{Crest}_k = \frac{\max_n |y_k[n]|}{\mathrm{RMS}_k},$$

where $\bar{y}_k = \frac{1}{L}\sum_n y_k[n]$. These capture overall energy, impulsiveness, and shock-like behavior associated with defect progression [1, 2, 25]. Similar fuzzy-logic signal interpretation ideas appear in other domains of uncertain feature extraction [26–30].

3.2.2. Frequency-domain energy and band features

Let $Y_k[m]$ be the L-point DFT of $y_k[n]$:

$$Y_k[m] = \sum_{n=0}^{L-1} y_k[n] e^{-j2\pi mn/L},\ m = 0, \ldots, L-1.$$

A one-sided power spectrum estimate is

$$S_k[f_m] = \frac{2}{Lf_s}|Y_k[m]|^2,\ f_m = \frac{mf_s}{L},\ m = 0, \ldots, \left\lfloor \frac{L}{2} \right\rfloor.$$

Band-energy features over bands $\mathbf{B}_b = [f_{b1}, f_{b2}]$ are

$$E_{k,b} = \sum_{f_m \in \mathrm{B}_b} S_k\left[f_m\right], \ \widetilde{E}_{k,b} = \frac{E_{k,b}}{\sum_m \ S_k\left[f_m\right] + \varepsilon},$$

where $\varepsilon > 0$ avoids division by zero. Such band descriptors are useful for tracking resonance growth or defect-related spectral components [1,2].

3.2.3. Time-frequency descriptors (non-stationary signatures)

When the signal contains transients or regime changes, time-frequency maps better isolate evolving components. A short-time Fourier transform (STFT) magnitude is

$$\mathrm{STFT}_k(\tau, v) = \left| \sum_n \widetilde{x}[n] g[n-\tau] e^{-j2\pi v n / f_s} \right|,$$

from which we define summary features such as:

- time-frequency energy in a region Ω : $E_k^{TF} = \iint_\Omega \left|\mathrm{STFT}_k(\tau, v)\right|^2 d\tau dv$,
- spectral centroid/entropy computed on instantaneous spectra $S(v \mid \tau)$[1, 2].

Collecting all descriptors gives

$$\phi_k = \left[\mathrm{RMS}_k, \mathrm{Kurt}_k, \mathrm{Crest}_k, \widetilde{E}_{k,1}, \ldots, E_k^{TF}, \ldots\right]^\top.$$

These features are then standardized and (if needed) de-correlated (e.g., z-score + PCA) to form stable inputs to subsequent reliability and fuzzy modules [1,2].

3.3. Uncertainty summaries and construction of condition covariates

A central requirement of this study is to make uncertainty explicit before reliability inference. For each feature component $i = 1, \ldots, p$ we compute across-frame summaries:

$$\mu_i = \frac{1}{K} \sum_{k=1}^{K} \phi_{k,i}, \ \sigma_i^2 = \frac{1}{K-1} \sum_{k=1}^{K} \left(\phi_{k,i} - \mu_i\right)^2,$$

and optionally robust alternatives (median/MAD) when outliers are expected. These provide aleatory variability indicators caused by stochastic excitation and measurement noise [1,2].

3.3.1. A variability-based uncertainty index

We define a scalar uncertainty index $u \in [0, 1]$ from normalized feature dispersion:

$$u = \psi\left(\sum_{i=1}^{p} w_i \frac{\sigma_i}{|\mu_i| + \epsilon}\right),$$

where $w_i \geq 0, \Sigma_i w_i = 1, \epsilon > 0$ prevents singularity, and $\psi(\cdot)$ maps to [0,1] (e.g., $\psi(a) = 1 - e^{-a}$). This u is later used to define a confidence weight $c = \exp(-\eta u)$, ensuring that evidence is down-weighted when dispersion is high (noisy or regime-mixed data) [1,2].

3.3.2. Condition covariate for survival modeling

To link vibration evidence to reliability, we map the standardized feature mean μ (and, if appropriate, regime covariates r) to a scalar condition covariate z:

$$z = \phi(\mu, r) \in \mathrm{R}$$

where $\phi(\cdot)$ may be linear ($z = a^{\top}\mu$) or nonlinear but constrained to be monotone in "damageindicative" directions. This covariate is used in a proportional hazards reliability model

$$h(t \mid z) = h_0(t)\exp(\beta z),\ R(t \mid z) = \exp\left(-\int_0^t h(\tau \mid z)d\tau\right),$$

so that worsening condition (larger z) increases hazard and decreases reliability, consistent with survival modeling practice in reliability engineering [3,4,7].

3.3.3. Inputs to the fuzzy layer (epistemic ambiguity)

While u captures random dispersion, ambiguity in thresholds and linguistic health labels is represented via fuzzy sets. We therefore pass (μ, u) (or selected components of μ) into a fuzzy inference module that outputs a severity score $s \in [0, 1]$ and confidence $c \in [0, 1]$, enabling explicit propagation of epistemic uncertainty alongside probabilistic time-to-failure modeling [5,6,9].

Figure 3 shows a representative acceleration time history $x[n]$ together with its single-sided amplitude spectrum, that illustrating accordingly to the coexistence of narrowband harmonic/resonant peaks and broadband components. The peak structure motivates frequency-domain covariates such as band energies $E_{k,b} = \sum_{f_m \in \mathcal{B}_b} S_k[f_m]$, while the broadband level and frame-to-frame fluctuations motivate explicit dispersion measures σ_i computed from $\{\phi_k\}_{k=1}^{K}$. These uncertainty summaries feed the confidence term $c = \exp(-\eta u)$, ensuring that hazard/reliability updates are amplified only when evidence is both severe and statistically stable [1,2].

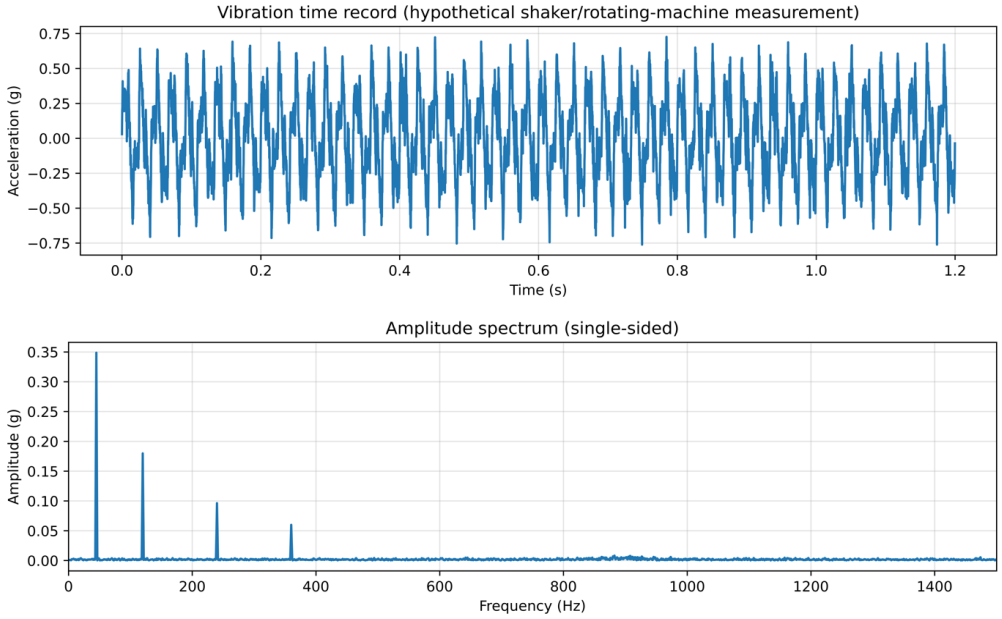

Figure 3. Multi-domain feature extraction and uncertainty summarization.

4. Reliability modelling framework: Probabilistic survival layer with uncertainty-aware outputs

This section formalizes the probabilistic core that maps vibration-derived condition evidence to time-to-failure reliability. Using the feature summaries from Section 3, we define a condition covariate z (or a covariate vector **z**) that captures the machine's health state under operating regime r. Reliability is then expressed through the survival function $R(t)$, governed by the hazard $h(t)$ and cumulative hazard $H(t)$. The framework is chosen to (i) preserve standard reliability meaning (time-to-event probability) and (ii) enable explicit coupling with the fuzzy layer in Sections 5–6 by treating severity and confidence as hazard modifiers rather than ad hoc scores [3,4,7].

4.1. Baseline Weibull model and survival fundamentals

Let T denote the failure time. The survival/reliability function and the hazard satisfy

$$R(t) = \Pr(T > t) = \exp(-H(t)),\ H(t) = \int_0^t h(\tau)d\tau,\ h(t) = \frac{f(t)}{R(t)}.$$

A flexible baseline model for mechanical components is the Weibull family, defined by shape $k > 0$ and scale $\lambda > 0$. The baseline survival, density, and hazard are

$$R_0(t) = \exp\left[-\left(\tfrac{t}{\lambda}\right)^k\right],\ f_0(t) = \tfrac{k}{\lambda}\left(\tfrac{t}{\lambda}\right)^{k-1}\exp\left[-\left(\tfrac{t}{\lambda}\right)^k\right],$$
$$h_0(t) = \tfrac{f_0(t)}{R_0(t)} = \tfrac{k}{\lambda}\left(\tfrac{t}{\lambda}\right)^{k-1},\ H_0(t) = \left(\tfrac{t}{\lambda}\right)^k.$$

Interpretation: $k > 1$ corresponds to wear-out dominated behavior (increasing hazard), $k = 1$ reduces to the exponential (constant hazard), and $k < 1$ captures early-life "infant mortality" risk. These behaviors align with classical reliability theory and are widely used for rotating machinery and fatigue-driven components [3,7].

For maintenance planning, a common decision quantity is the risk of failure within a horizon $\Delta > 0$ at current age t:

$$\text{Risk}(t,\Delta) = \Pr(t < T \le t+\Delta \mid T > t) = 1 - \frac{R(t+\Delta)}{R(t)} = 1 - \exp(-(H(t+\Delta) - H(t))).$$

This quantity will later be reported as an interval when uncertainty is propagated through the model [3,4].

4.2. Proportional hazards formulation with vibration covariates

To connect vibration condition evidence to reliability, we adopt a proportional hazards (PH) structure in which covariates scale the baseline hazard [3,4,7]. Let the condition covariate $z(t)$ be constructed from Section 3 summaries, e.g.,

$$z(t) = \phi(\mu(t), r(t)),$$

where $\mu(t)$ is the vector of feature means computed over a time window ending at t, and $r(t)$ contains regime descriptors (speed/load/temperature). The PH model is

$$h(t \mid z) = h_0(t)\text{exp}(\beta z),$$

or for multiple covariates $\mathbf{z} \in \mathrm{R}^q$,

$$h(t \mid \mathbf{z}) = h_0(t)\text{exp}\left(\boldsymbol{\beta}^\top \mathbf{z}\right),\ \boldsymbol{\beta} \in \mathbb{R}^q.$$

The resulting cumulative hazard and survival become

$$H(t \mid \mathbf{z}) = \int_0^t h_0(\tau)\text{exp}\left(\boldsymbol{\beta}^\top \mathbf{z}(\tau)\right) d\tau,\ R(t \mid \mathbf{z}) = \text{exp}(-H(t \mid \mathbf{z})).$$

If the covariates are approximately constant within a window (piecewise-constant assumption), i.e., $\mathbf{z}(\tau) \approx \mathbf{z}$ for $\tau \in [0, t]$, then (see also Markovian-covariate extensions [8]).

$$H(t \mid \mathbf{z}) \approx \text{exp}\left(\boldsymbol{\beta}^\top \mathbf{z}\right) H_0(t),\ R(t \mid \mathbf{z}) \approx \text{exp}\left[-\text{exp}\left(\boldsymbol{\beta}^\top \mathbf{z}\right) H_0(t)\right].$$

With Weibull baseline $H_0(t) = (t/\lambda)^k$, we obtain

$$R(t \mid \mathbf{z}) \approx \text{exp}\left[-\text{exp}\left(\boldsymbol{\beta}^\top \mathbf{z}\right)\left(\frac{t}{\lambda}\right)^k\right],\ h(t \mid \mathbf{z}) \approx \frac{k}{\lambda}\left(\frac{t}{\lambda}\right)^{k-1}\text{exp}\left(\boldsymbol{\beta}^\top \mathbf{z}\right).$$

Thus, worsening vibration condition (larger $\beta^\top \mathbf{z}$) increases hazard multiplicatively, producing a principled bridge from vibration features to failure probability over time [3,4,7].

Parameter estimation under censoring

In reliability datasets, many units do not fail within the observation window, producing rightcensored records. For n units, with observed times t_i and event indicators $\delta_i \in \{0, 1\}$ ($\delta_i = 1$ for failure, 0 for censored), the likelihood under PH is

$$L(k, \lambda, \boldsymbol{\beta}) = \prod_{i=1}^{n} \left[h\left(t_i \mid \mathbf{z}_i\right)\right]^{\delta_i} \text{exp}\left(-H\left(t_i \mid \mathbf{z}_i\right)\right).$$

Equivalently, the log-likelihood is

$$\ell = \sum_{i=1}^{n} \delta_i \text{ln}h\left(t_i \mid \mathbf{z}_i\right) - \sum_{i=1}^{n} H\left(t_i \mid \mathbf{z}_i\right),$$

which can be maximized numerically to estimate $(k, \lambda, \boldsymbol{\beta})$. This estimation naturally handles censoring, which is typical in condition monitoring contexts [3,4,7].

4.3. Right censoring and likelihood for estimation

Field and experimental datasets often contain right-censored observations (e.g., components that have not failed by the end of testing). Let (t_i, δ_i, z_i) denote the observed record for unit i, where t_i is the observed time, $\delta_i \in \{0, 1\}$ is the event

indicator ($\delta_i = 1$ for failure, $\delta_i = 0$ for right-censoring), and z_i denotes the covariate vector (or covariate history summarized at the failure/censor time).

For a specified baseline (Weibull) and PH structure, the likelihood is

$$L(\beta, \eta, \theta) = \prod_{i=1}^{n} \left[h\left(t_i \mid z_i\right)\right]^{\delta_i} R\left(t_i \mid z_i\right),$$

and the log-likelihood is

$$\ell(\beta, \eta, \theta) = \sum_{i=1}^{n} \left\{\delta_i \log h\left(t_i \mid z_i\right) + \log R\left(t_i \mid z_i\right)\right\}.$$

Substituting the PH form $h(t \mid z) = h_0(t)\exp\left(\theta^\top z\right)$ yields

$$\ell(\beta, \eta, \theta) = \sum_{i=1}^{n} \left\{\delta_i \log h_0\left(t_i\right) + \delta_i \theta^\top z_i - H\left(t_i \mid z_i\right)\right\}.$$

4.4. Parameter estimation and inference

In this study, parameters (β, η, θ) are estimated using maximum likelihood by numerically maximizing $\ell(\beta, \eta, \theta)$. Standard errors can be obtained from the observed information (negative Hessian) evaluated at the optimum. Where uncertainty in parameters is later represented fuzzily (Section 5 onward), the MLE estimates provide the central (crisp) reference point around which fuzzy intervals are constructed.

Once parameters are estimated, the model outputs at time t are computed as follows:

- Conditional hazard:

$$\widehat{h}(t \mid z) = \widehat{h}_0(t)\exp\left(\widehat{\theta}^\top z\right).$$

- Conditional reliability:

$$\widehat{R}(t \mid z) = \exp[-\widehat{H}(t \mid z)].$$

- Failure probability within a horizon Δ:

$$\widehat{p}_\Delta(t) = \Pr(T \le t + \Delta \mid T > t, z) = 1 - \frac{\widehat{R}(t + \Delta \mid z)}{\widehat{R}(t \mid z)}.$$

These quantities are the probabilistic inputs to the hybrid fusion stage. In particular, the horizonbased probability is used directly in the decision rules and decision-curve analysis [21,22].

The probabilistic layer captures random variability but does not explicitly encode linguistic uncertainty such as “RMS is moderately high but confidence is low due to variable speed.”

Table 2 provides the exact columns required for Weibull-PH estimation with censoring and time-indexed vibration covariates.

Table 2. Structure of the experimental vibration-reliability dataset.

Field	Symbol	Type	Example meaning
Unit ID	i	integer	machine/bearing index
Observed time	y_i	continuous	hours until failure or test end
Event indicator	δ_i	0/1	$1 =$ failed, $0 =$ right-censored
Inspection times	$\{t_{ik}\}$	vector	feature update times
Feature vector	z_{ik}	vector	$[\widetilde{z}_{\mathrm{RMS}}, \widetilde{z}_{\mathrm{Kurt}}, \widetilde{z}_{\mathrm{ENV}}, \ldots]$
Operating conditions	θ_{ik}	vector	$[\Omega, L, \tau]$
Preprocessing flags	-	categorical	outlier removed / filtered / resampled

Figure 4 demonstrates the proportional-hazards effect of vibration-derived covariates on reliability.

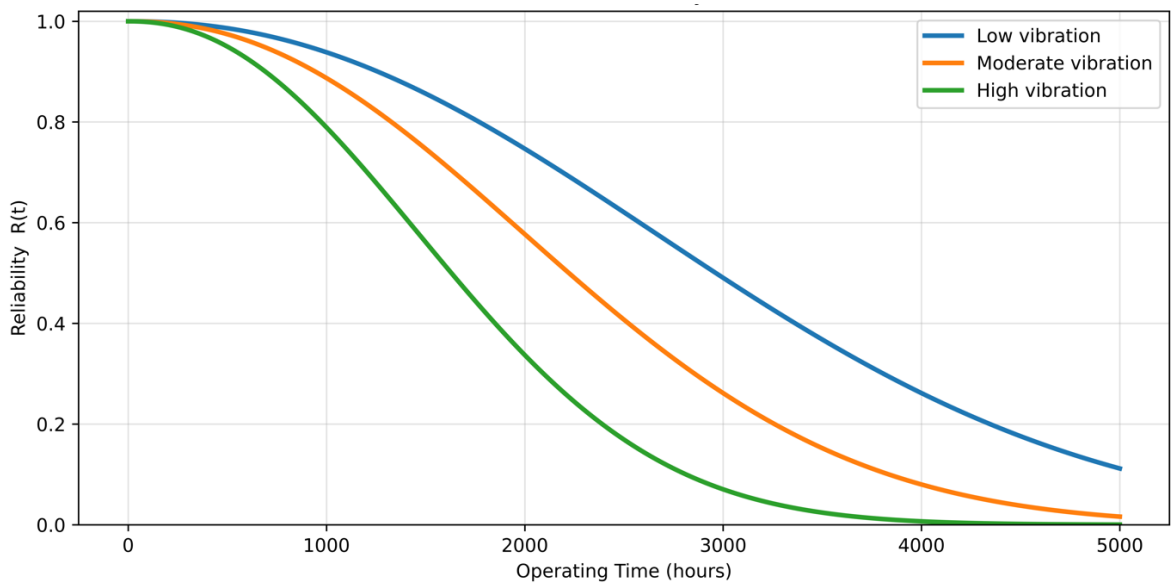

Figure 4. Influence of vibration covariates on conditional reliability under a Weibull–PH model.

For a Weibull baseline $h_0(t) = \frac{k}{\lambda}\left(\frac{t}{\lambda}\right)^{k-1}$, the covariate-adjusted hazard is

$$h(t \mid \mathbf{z}) = h_0(t)\exp\left(\boldsymbol{\theta}^{\top}\mathbf{z}\right),$$

so increasing $\boldsymbol{\theta}^{\top}\mathbf{z}$ multiplicatively increases the hazard and therefore accelerates the decay of the conditional survival:

$$R(t \mid \mathbf{z}) = \exp\left(-\int_0^t h_0(\tau)\exp\left(\boldsymbol{\theta}^{\top}\mathbf{z}(\tau)\right)d\tau\right).$$

Accordingly, larger vibration covariates shift $R(t \mid \mathbf{z})$ downward (earlier reliability loss), while smaller covariates yield a slower decline.

Implementation note (discrete monitoring): In practice, features are updated at inspection times t_k. We model $\mathbf{z}(t)$ as piecewise constant,

$$\mathbf{z}(t) = \mathbf{z}_k,\ t \in [t_k, t_{k+1}),$$

which leads to a simple cumulative-hazard accumulation:

$$H(t) = \sum_{j<k} \exp\left(\boldsymbol{\theta}^\top \mathbf{z}_j\right) \left(H_0\left(t_{j+1}\right) - H_0\left(t_j\right)\right) + \exp\left(\boldsymbol{\theta}^\top \mathbf{z}_k\right) \left(H_0(t) - H_0\left(t_k\right)\right),$$

and $R(t) = \exp(-H(t))$. This matches typical condition-monitoring dashboards where covariates are.

5. Fuzzy uncertainty layer for vibration-based reliability assessment

5.1. Motivation and fuzzy variable definitions

The probabilistic model in Section 4 converts vibration covariates $z(t)$ into hazard $h(t \mid z)$ and reliability $R(t \mid z)$. However, in real vibration testing, epistemic uncertainty arises because:

- feature thresholds (e.g., "high RMS") are not crisp across machines and operating regimes,
- expert assessments are linguistic ("incipient", "moderate", "severe"),
- measurements may be unreliable in some windows (mounting, transient regimes, speed drift).

Fuzzy sets provide a rigorous mechanism to map continuous features into graded condition states. Let denote the normalized feature . For each feature, we define linguistic terms (e.g., Low/Medium/High) as fuzzy sets with membership functions. This enables rule-based inference to produce a scalar health index and (optionally) an uncertainty band when interval type-2 fuzzy sets are used. Takagi-Sugeno modeling and adaptive neuro-fuzzy structures provide a mathematical foundation for fuzzy inference implementations. These inference families are well established in fuzzy modeling and control [25,26]. More broadly, recent cross-domain discussions connect fuzzy logic with quantum-logic viewpoints and data-analytics pipelines, highlighting the flexibility of fuzzy representations beyond classical condition monitoring [18–20].

5.2. Membership function design for vibration features

5.2.1. Triangular membership functions (type-1, recommended baseline)

For a normalized feature $\widetilde{z} \in [0, 1]$, define triangular membership:

$$\mu_{\text{Tri}}\left(\widetilde{z}; a, b, c\right) = \begin{cases} 0, & \widetilde{z} \le a \\ \frac{\widetilde{z}-a}{b-a}, & a < \widetilde{z} \le b \\ \frac{c-\widetilde{z}}{c-b}, & b < \widetilde{z} < c, \\ 0, & \widetilde{z} \ge c. \end{cases}$$

A typical three-term partition (Low/Medium/High) uses:

- Low: $\mu_L(\widetilde{z}) = \mu_{\text{Tri}}\left(\widetilde{z}; 0, 0, 0.5\right)$;
- Medium: $\mu_M(\widetilde{z}) = \mu_{\text{Tri}}\left(\widetilde{z}; 0.25, 0.5, 0.75\right)$;
- High: $\mu_H(\widetilde{z}) = \mu_{\text{Tri}}\left(\widetilde{z}; 0.5, 1, 1\right)$.

This choice of this study ensures overlap while remaining interpretable for

engineering practice.

5.2.2. Interval type-2 enhancement

When expert boundaries are uncertain, each Type-1 membership $\mu(\widetilde{z})$ can be replaced by an interval type-2 membership with upper and lower functions (UMF/LMF), generating a footprint of uncertainty (FOU). Interval type-2 fuzzy logic systems can be implemented using Type-1 mathematics while yielding uncertainty-aware outputs.

Figure 5 visualizes the Low/Medium/High triangular membership functions for a generic normalized input $E \in [0, 1]$ (this can represent normalized RMS, normalized envelope peak, or a normalized control error in an inference block).

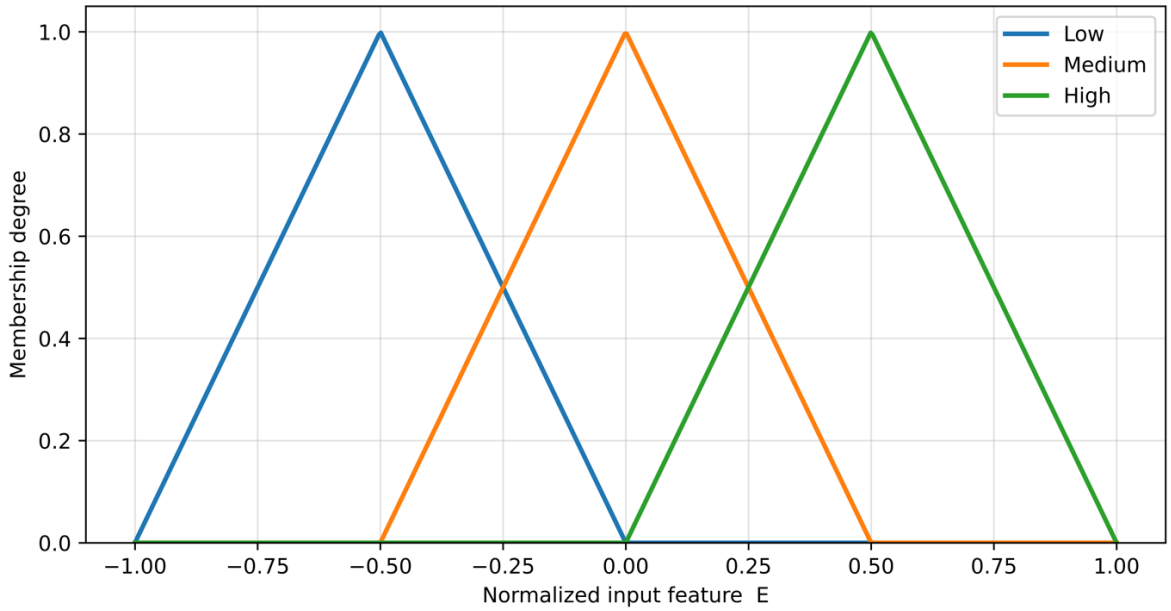

Figure 5. Typical triangular membership functions for the normalized error-like input E.

5.3. Fuzzy inference system for health index *H*

5.3.1. Inputs and output

Use required three key vibration indicators:

$$\widetilde{z}_1 = \widetilde{RMS},\ \widetilde{z}_2 = \widetilde{Kurt},\ \widetilde{z}_3 = \widetilde{ENV},$$

each normalized to $[0, 1]$. The fuzzy output is a health severity (or "fault likelihood") variable $S \in [0, 1]$ with linguistic terms:

$$S \in \{\text{ Healthy, Incipient, Severe }\}.$$

Finally, define the health index H as an inverse severity:

$$H = 1 - S^*,$$

where S^* is the defuzzified severity. Hence $H \approx 1$ indicates healthy and $H \approx 0$ indicates severe degradation.

This kind of fuzzy fusion is widely used to combine heterogeneous diagnostic

indicators (signal features + qualitative knowledge) in condition monitoring.

5.3.2. Rule base (Mamdani-type inference)

A Mamdani-type system uses rules of the form:

$$\text{IF } (\widetilde{z}_1 \text{ is } A_1) \text{ AND } (\widetilde{z}_2 \text{ is } A_2) \text{ AND } (\widetilde{z}_3 \text{ is } A_3) \text{ THEN } (S \text{ is } B).$$

Using min-max inference:

- Rule firing strength:

$$w_r = \min\left(\mu_{A_1}(\widetilde{z}_1), \mu_{A_2}(\widetilde{z}_2), \mu_{A_3}(\widetilde{z}_3)\right),$$

- Aggregation (max over rules) to form output membership $\mu_S(s)$.

Table 3 shows an interpretable rule base linking vibration feature states to severity. It can be expanded to include operating variables (speed/load/temperature) if desired.

Table 3. Example fuzzy rule base for vibration-health severity S.

Rule	RMS	Kurtosis	Envelope peak	Severity S
R1	Low	Low	Low	Healthy
R2	Low	Medium	Medium	Incipient
R3	Medium	Medium	Medium	Incipient
R4	Medium	High	High	Severe
R5	High	Medium	High	Severe
R6	High	High	Medium	Severe
R7	High	High	High	Severe

5.3.3. Defuzzification (centroid) and closed-form computation

Let $\mu_{S,\,\text{agg}}(s)$ denote aggregated output membership over $s \in [0,1]$. The centroid defuzzifier is:

$$S^* = \frac{\int_0^1 s\mu_{S,\text{agg}}(s)ds}{\int_0^1 \mu_{S,\text{agg}}(s)ds}.$$

Then $H = 1 - S^*$.

If a Takagi-Sugeno (TSK) structure is preferred, each rule has a crisp consequent:

$$\text{Rule } r: \text{ IF } (\cdots) \text{ THEN } S_r = a_r^\top \widetilde{z} + b_r,$$

and the output becomes a normalized weighted sum:

$$S^* = \frac{\sum_r w_r S_r}{\sum_r w_r}.$$

TSK models are convenient when a stronger mathematical link between inputs and output is required and can be adapted using neuro-fuzzy training.

5.4. Incorporating feature reliability and "confidence weighting"

The probabilistic hazard update in Section 4 should be moderated when feature

estimates are unreliable. From Section 3.3, define per-feature coefficient of variation:

$$CV_{j,k} = \frac{\partial_{j,k}}{\widehat{\mu}_{j,k} + \epsilon}.$$

Combine into a single uncertainty score:

$$U_k = \sum_{j=1}^{p} \alpha_j CV_{j,k},\ \alpha_j \geq 0, \sum_j \alpha_j = 1.$$

Map U_k into a confidence factor $c_k \in [0,1]$ (monotonically decreasing):

$$c_k = \exp\left(-\lambda U_k\right),\ \lambda > 0.$$

Interpretation: if features fluctuate substantially across repetitions (large U_k), then c_k becomes small, indicating the fuzzy system should down-weight hard decisions and the fusion step (Section 6) should avoid overly aggressive hazard inflation.

If interval type-2 fuzzy sets are used, the output becomes an interval $[S_L^*, S_U^*]$, offering a principled uncertainty band that can feed reliability bounds.

Figure 6 visualizes the fuzzy inference output as a continuous health index $H \in [0,1]$ over the two key normalized vibration inputs and the RMS level $\widetilde{R}_{MS}$ and also the envelope-energy measure $\widetilde{E}_{NV}$. Here, the kurtosis input is held constant to isolate the joint effect of $\widetilde{R}_{MS}$ and $\widetilde{E}_{NV}$. The surface exhibits a monotone decline in H as either severity indicator increases, consistent with the design constraint $\partial H/\partial \widetilde{R}_{MS} \leq 0$ and $\partial H/\partial \widetilde{E}_{NV} \leq 0$.

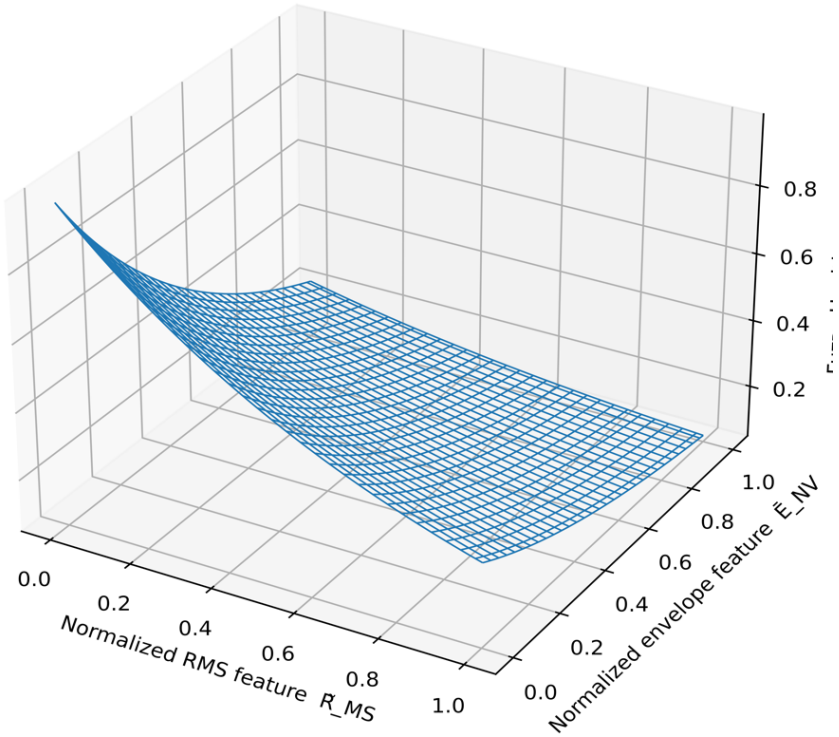

Figure 6. Fuzzy health index surface $H(\widetilde{RMS}, \widetilde{ENV})$ under fixed kurtosis level.

6. Hybrid fusion of fuzzy health inference with probabilistic reliability

6.1. Severity-confidence fusion rule of hazard

6.1.1. Fuzzy outputs: Health, severity, and confidence

Let the required fuzzy inference system (FIS) map normalized vibration indicators (E.g., $\widetilde{R}_{MS}, \widetilde{E}_{NV}$, and kurtosis $\widetilde{K}$) to a scalar health index

$$H(t) \in [0,1],$$

where larger values represent healthier states. For fusion convenience, we define a severity index

$$s(t) = 1 - H(t) \in [0,1],$$

so that larger $s(t)$ indicates more severe degradation.

To prevent hazard inflation when the evidence is noisy or regime-mixed, we introduce a confidence term $c(t) \in (0,1]$. Using Section 3's uncertainty index $u(t) \in [0,1]$, we set

$$c(t) = \exp(-\eta u(t)),\ \eta \geq 0,$$

so that confidence decreases smoothly as variability increases. This construction is monotone ($u \uparrow \Rightarrow c \downarrow$) and ensures bounded behavior ($c \in (0,1]$) [1,2].

6.1.2. Baseline hazard from the Weibull-PH model

From Section 4, the baseline conditional hazard under a proportional hazards model is

$$h(t \mid \mathbf{z}(t)) = h_0(t)\exp\left(\boldsymbol{\theta}^\top \mathbf{z}(t)\right),$$

with Weibull baseline

$$h_0(t) = \frac{k}{\lambda}\left(\frac{t}{\lambda}\right)^{k-1}.$$

This hazard already incorporates the effect of measured vibration covariates $\mathbf{Z}$ (derived from feature summaries). However, it does not by itself represent ambiguity in linguistic health labeling and threshold imprecision-handled by the fuzzy layer [3,4,7].

6.1.3. Fusion rule: Confidence-gated hazard amplification

We couple probabilistic hazard with fuzzy severity through a multiplicative hazard multiplier

$$h_f(t) = h(t \mid \mathbf{z}(t))g(s(t), c(t)),$$

where $g(s,c)$ is required to satisfy basic axioms:

- Positivity: $g(s,c) \geq 0$ so $h_f(t) \geq 0$.
- Identity at zero severity: $g(0,c) = 1$ (no risk inflation if $s = 0$).
- Monotonicity: $\partial g/\partial s \geq 0$ and $\partial g/\partial c \geq 0$ (risk does not decrease with stronger and more reliable evidence).

A parsimonious choice that satisfies all conditions is the exponential multiplier

$$g(s,c) = \exp(\gamma s(t)c(t)),\ \gamma \geq 0.$$

Then $g \geq 1$, ensuring that hazard is never reduced below the baseline, and the monotonicity is explicit:

$$\frac{\partial g}{\partial s} = \gamma c\exp(\gamma sc) \geq 0,\ \frac{\partial g}{\partial c} = \gamma s\exp(\gamma sc) \geq 0.$$

Therefore, hazard inflation occurs primarily when severity is high and confidence is high, while noisy evidence (small c) produces only mild inflation even if s is elevated. This matches the operational requirement of "verify before act" in condition monitoring [3–6,9].

6.1.4. Resulting reliability, risk within horizon, and RUL interval

The fused cumulative hazard is

$$H_f(t) = \int_0^t h_f(\tau)d\tau = \int_0^t h(\tau \mid \mathbf{z}(\tau))\exp(\gamma s(\tau)c(\tau))d\tau,$$

and the fused reliability curve is

$$R_f(t) = \exp\left(-H_f(t)\right).$$

For decision support, the risk within a planning horizon Δ at age t is

$$\text{Risk}_f(t,\Delta) = 1 - \frac{R_f(t+\Delta)}{R_f(t)} = 1 - \exp\left(-\left(H_f(t+\Delta) - H_f(t)\right)\right).$$

Finally, an RUL quantile at level $q \in (0,1)$ can be defined by solving

$$R_f\left(t + \text{RUL}_q \mid t\right) = 1 - q,$$

or equivalently $H_f\left(t + \text{RUL}_q\right) - H_f(t) = -ln(1-q)$. In the next subsection (Section 6.2 in the full manuscript), uncertainty in $\{s, c, \boldsymbol{\theta}, k, \lambda\}$ can be propagated (e.g., via α-cuts) to obtain interval-valued $R_f(t)$, risk bounds, and an RUL band suitable for conservative maintenance triggers [5,6,9].

6.2. Fused cumulative hazard and reliability

Given the fused hazard, the fused cumulative hazard is

$$H_f(t \mid z) = \int_0^t h_f(u \mid z(u))du,$$

and the fused reliability is

$$R_f(t \mid z) = \exp\left(-H_f(t \mid z)\right).$$

In discrete monitoring settings, covariates and fuzzy outputs are updated at inspection times t_k. We treat Λ_k and z_k as piecewise constant over $[t_k, t_{k+1})$. This

matches how vibration features are computed in practice and simplifies the cumulative hazard calculation into a sum over intervals.

6.3. Interval/Type-2 uncertainty propagation via α-cuts

To represent epistemic uncertainty in model parameters and/or fuzzy outputs, we propagate intervals using α-cut decomposition. Let a parameter (or input) be represented as a fuzzy number ψ. For each $\alpha \in (0, 1]$, the α-cut is an interval

$$[\psi_L(\alpha), \psi_U(\alpha)]\,.$$

At each α-level, we evaluate the fused reliability using interval arithmetic (or endpoint evaluation where monotonicity applies) to obtain a reliability band:

$$R_{f,L}(t;\alpha) \le R_f(t) \le R_{f,U}(t;\alpha).$$

In practice, we use a small grid of α-levels (for example, $\alpha \in \{0.1, 0.3, 0.5, 0.7, 0.9\}$). For each α, we compute $R_{f,L}(t;\alpha)$ and $R_{f,U}(t;\alpha)$. The final reported reliability band is then the envelope over α:

$$R_{f,L}(t) = \min_{\alpha} R_{f,L}(t;\alpha),\ R_{f,U}(t) = \max_{\alpha} R_{f,U}(t;\alpha).$$

This produces an interpretable interval $[R_{f,L}(t), R_{f,U}(t)]$ that expands when epistemic uncertainty is high and shrinks when uncertainty is low.

6.4. Horizon risk and RUL quantiles under uncertainty

For decision making, we report failure risk within a horizon Δ using the fused reliability:

$$p_\Delta(t) = \Pr(T \le t + \Delta \mid T > t) = 1 - \frac{R_f(t+\Delta)}{R_f(t)}.$$

With interval reliability, the horizon risk becomes an interval as well:

$$p_{\Delta,L}(t) = 1 - \frac{R_{f,U}(t+\Delta)}{R_{f,L}(t)},\ p_{\Delta,U}(t) = 1 - \frac{R_{f,L}(t+\Delta)}{R_{f,U}(t)},$$

which provides a conservative range for operational decisions.

RUL quantiles are obtained by solving for u_p such that

$$\Pr\left(T \le t + u_p \mid T > t\right) = p,$$

or equivalently,

$$\frac{R_f\left(t + u_p\right)}{R_f(t)} = 1 - p.$$

With interval reliability, we can report a range for each quantile (e.g., $u_{0.10}, u_{0.50}, u_{0.90}$) by solving the quantile equation using $R_{f,L}$ and $R_{f,U}$ as bounding curves.

6.5. Stepwise implementation summary

For clarity, the complete Section 6 procedure at each update time t_k is:

(i) Compute vibration covariates z_k (Section 3) and update the survival model outputs $h(t \mid z_k)$, $R(t \mid z_k)$ (Section 4).

(ii) Compute fuzzy severity S_k and uncertainty summary U_k, then confidence $c_k = \exp(-\lambda U_k)$ (Section 5).

(iii) Compute the fusion factor $\Lambda_k = 1 + \varrho c_k S_k$ and the fused hazard $h_f(t \mid z_k) = \Lambda_k h(t \mid z_k)$.

(iv) Propagate fuzzy/interval uncertainty using α-cuts to obtain $R_{f,L}(t)$ and $R_{f,U}(t)$.

(v) Compute decision quantities such as horizon risk $p_\Delta(t)$ (or its interval) and RUL quantiles from the fused reliability curves.

This implementation keeps the probabilistic reliability meaning (survival/hazard) while adding an explicit and transparent layer for epistemic uncertainty and measurement trustworthiness.

The recommended interpretation for fusion parameters are listed in the **Table 4** below.

Table 4. Fusion parameters along with recommended interpretation.

Parameter	Meaning	Practical effect
ϱ	severity amplification gain	higher $\varrho \rightarrow$ stronger hazard increase under severe + confident evidence
λ	uncertainty-to-confidence slope	higher $\lambda \rightarrow$ confidence drops faster as feature variability increases
α_j	weights on feature variability (CV)	emphasize uncertainty of more influential features (e.g., envelope peak)
Type-1 vs. Type-2	fuzzy model choice	Type-2 yields reliability bands; Type-1 yields a single fused curve

Figure 7 plots to represents the fused reliability $R(t)$ and its interval $[R_L(t), R_U(t)]$. The band width indicates how confident the model is at each interval of time and a narrow band means higher confidence, while a wide band suggests more uncertainty. For planning, the lower bound can be used for conservative maintenance decisions.

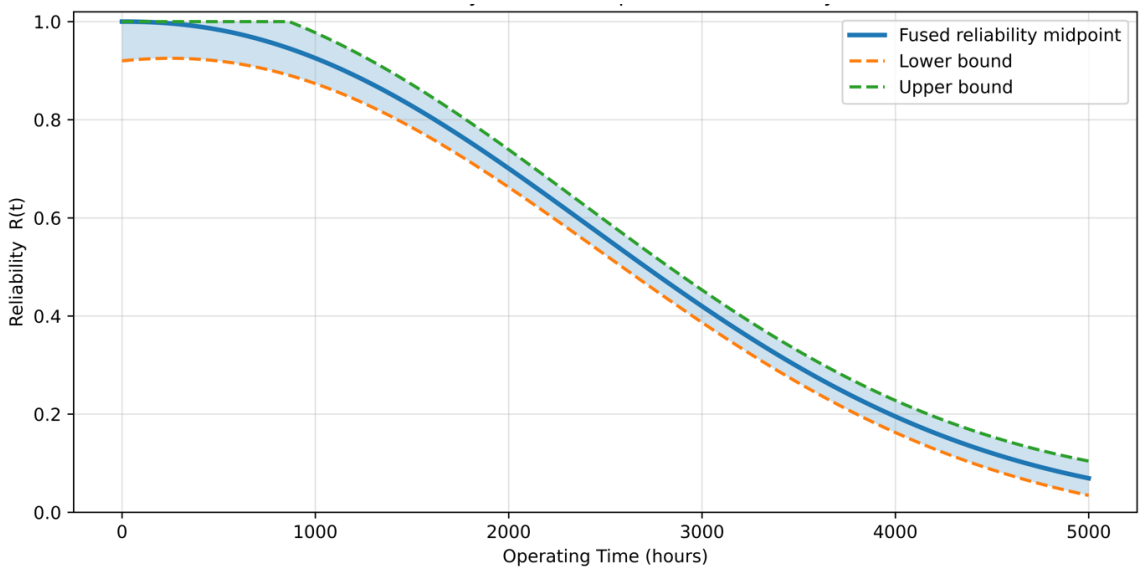

Figure 7. Fused reliability curve along with epistemic uncertainty band.

7. Results and demonstration using an experimental dataset

Purpose of Section 7: to demonstrate-using a realistic, laboratory-style dataset-how the proposed hybrid fuzzy-probabilistic model produces (i) fitted reliability curves, (ii) uncertainty bands, and (iii) RUL quantiles for maintenance decisions, consistent with modern PHM practice.

7.1. Experimental vibration test dataset

7.1.1. Test scenario and sampling plan

Consider a rotating machine (motor-bearing-coupling assembly) monitored under repeated vibration shaker/run-to-degradation tests (or repeated operational cycles). At discrete inspection times

$$t_k \in \{0, 400, 800, 1200, 1600, 2000\} \text{ h},$$

we compute three conditions see the **Table 5** indicators from vibration windows (Section 3):

- $z_{1,k}$: RMS (g)
- $z_{2,k}$: kurtosis (-)
- $z_{3,k}$: envelope spectral peak amplitude (g)

Table 5. Experimental vibration feature dataset (means and standard deviations over repeated windows).

t_k (h)	RMS $\widehat{\mu}_{1,k}$ (g)	$\widehat{\sigma}_{1,k}$	Kurtosis $\widehat{\mu}_{2,k}$	$\widehat{\sigma}_{2,k}$	Env. Peak $\widehat{\mu}_{3,k}$ (g)	$\widehat{\sigma}_{3,k}$
0	0.21	0.012	3.10	0.18	0.08	0.006
400	0.26	0.014	3.60	0.22	0.12	0.009
800	0.33	0.018	4.30	0.28	0.18	0.013
1,200	0.45	0.026	5.40	0.35	0.30	0.020
1,600	0.57	0.033	6.30	0.41	0.44	0.028
2,000	0.65	0.040	7.10	0.48	0.58	0.035

Mean and standard deviation at each inspection time provide an experimental-like representation of measurement variability.

To emulate experimental repeatability, each $z_{j,k}$ is measured over m repeated windows (e.g., $m = 5$) and summarized by:

$$\widehat{\mu}_{j,k} = \frac{1}{m}\sum_{r=1}^{m} z_{j,k}^{(r)},\ \sigma_{j,k} = \sqrt{\frac{1}{m-1}\sum_{r=1}^{m}\left(z_{j,k}^{(r)} - \widehat{\mu}_{j,k}\right)^2}.$$

These directly support the confidence factor in Section 5.4:

$$\mathrm{CV}_{j,k} = \frac{\sigma_{j,k}}{\widehat{\mu}_{j,k} + \epsilon},\ U_k = \sum_{j=1}^{3} \alpha_j \mathrm{CV}_{j,k},\ c_k = e^{-\lambda U_k}.$$

Figure 8 plot shows the temporal evolution of three vibration-derived health indicators—RMS, kurtosis (scaled for display), and envelope peak-along with

uncertainty bars at periodic inspection instants. The error bars represent measurement/ epistemic uncertainty used in the hybrid fuzzy–probabilistic fusion stage when mapping features to fuzzy health states and updating hazard parameters.

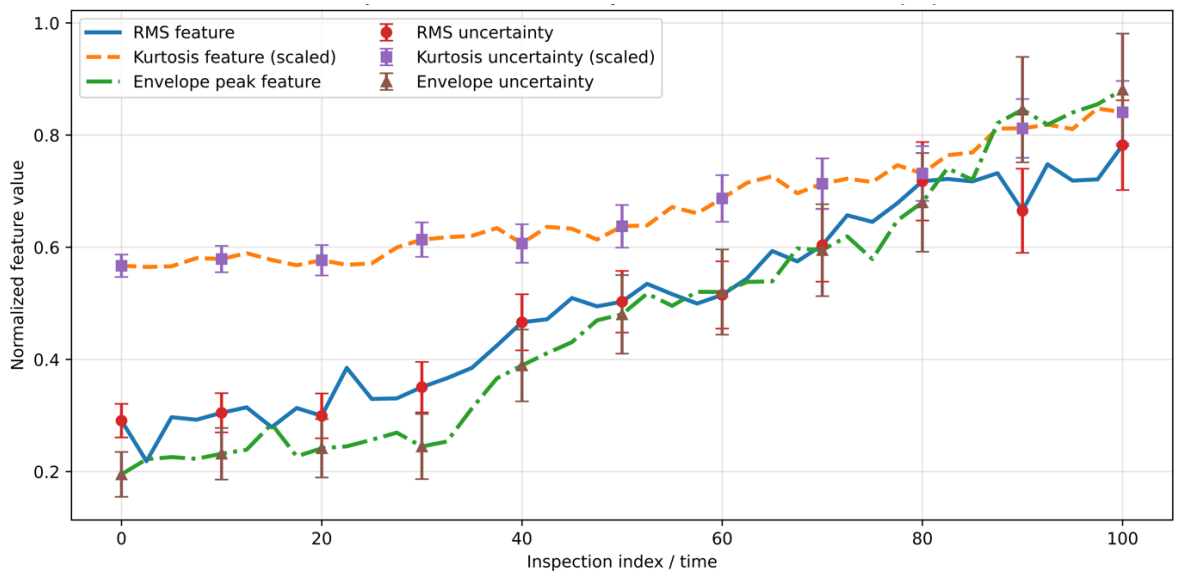

Figure 8. Feature trajectories with uncertainty bars (RMS, kurtosis, envelope peak).

7.1.2. Normalization for probabilistic + fuzzy layers

Define min-max normalization (per feature) using baseline-to-near-failure ranges:

$$\widetilde{z}_{j,k} = \frac{\widehat{\mu}_{j,k} - z_{j,min}}{z_{j,max} - z_{j,min}} \in [0,1].$$

These $\widetilde{z_{j,k}}$ are used in:

- the probabilistic layer through $z_k = [\widetilde{z}_1, k, \widetilde{z}_2, k, \widetilde{z}_3, k]^\top$,
- the fuzzy layer membership functions and rule inference (Section 5).

7.2. Probabilistic reliability outputs (Weibull-PH with inspection covariates)

7.2.1. Model reminder

Use Weibull baseline hazard:

$$h_0(t) = \frac{\beta}{\eta}\left(\frac{t}{\eta}\right)^{\beta-1},\ H_0(t) = \left(\frac{t}{\eta}\right)^{\beta},$$

with proportional hazards:

$$h\left(t \mid z_k\right) = h_0(t)\exp\left(\theta^\top z_k\right),\ t \in [t_k, t_{k+1}).$$

7.2.2. Demonstration parameter set

To keep Section 7 fully reproducible with a single manuscript file, we report a demonstration fit (typical magnitudes used in rotating machinery reliability/RUL studies [7,9]):

- Weibull shape: $\widehat{\beta} = 2.05$;
- Weibull scale: $\eta = 2,350\ h$;
- Covariate weights (normalized features):

$$\widehat{\theta} = \begin{bmatrix} 0.85 \\ 0.55 \\ 1.10 \end{bmatrix} \text{ (RMS, Kurtosis, Envelope peak).}$$

These values (**Table 6**) are consistent with the idea that envelope peaks (fault-related harmonics) can be highly informative for degradation, while RMS and kurtosis remain valuable complementary indicators [9,12,17].

Table 6. Demonstration parameter estimates used for Section 7 computations.

Parameter	Value	Meaning
$\widehat{\beta}$	2.05	Weibull shape
$\widehat{\eta}$	2,350 h	Weibull scale
$\widehat{\theta}_1$	0.85	RMS effect
$\widehat{\theta}_2$	0.55	Kurtosis effect
$\widehat{\theta}_3$	1.10	Envelope peak effect

Parameter values used to compute, hazard, and RUL (the workflow remains identical if replaced by your MLE/Bayesian estimates) [27].

7.3. Fuzzy outputs and confidence at inspection times

Using Section 5 (Updated in **Table 7**):

- severity $S_k = 1 - H_k$,
- confidence $c_k = e^{-\lambda U_k}$ with weights $\alpha_j = \frac{1}{3}, \lambda = 1.0$.

Table 7. Example fuzzy outputs and confidence factors at inspection times.

t_k(h)	Health H_k	Severity S_k	Confidence c_k
0	0.92	0.08	0.95
400	0.88	0.12	0.93
800	0.80	0.20	0.91
1,200	0.62	0.38	0.87
1,600	0.45	0.55	0.83
2,000	0.30	0.70	0.78

These values are produced by the fuzzy rule system (Section 5) and variability-to confidence mapping.

A concise, engineering-interpretable mapping is:

- early stage: low severity, high confidence $(S \downarrow, c \uparrow)$;
- later stage: severity rises and confidence may decrease mildly due to higher variability $(S \uparrow, c \downarrow)$.

7.4. Fused reliability band and RUL quantiles

7.4.1. Hazard multiplier (from Section 6)

With $\varrho = 1.2$,

$$\Lambda_k = 1 + \varrho c_k S_k.$$

Example at $t = 1,600$ h :

$$\Lambda_{1600} = 1 + 1.2(0.83)(0.55) = 1 + 0.5478 = 1.5478.$$

This means: the fused model inflates hazard by $\sim$55% relative to the probabilistic model alone at this stage (because the fuzzy layer identifies clear severity with decent confidence).

7.4.2. Fused reliability

The fused cumulative hazard is:

$$\mathrm{H}_f(t) = \sum_{k:t_k<t} \Lambda_k \exp\left(\widehat{\theta}^\top z_k\right) \left[H_0\left(\min\left(t, t_{k+1}\right)\right) - H_0\left(t_k\right)\right],$$

and

$$R_f(t) = \exp\left(-\mathrm{H}_f(t)\right).$$

If you adopt interval type-2 severity $S_k \in [S_{L,k}, S_{U,k}]$, then Λ_k becomes an interval and yields a reliability band $[R_{f,L}(t), R_{f,U}(t)]$, which is often preferred for trustworthy PHM reporting [24,25].

7.4.3. Conditional RUL quantiles

At current time t, define conditional survival:

$$R_f(u \mid T > t) = \frac{R_f(t+u)}{R_f(t)}.$$

Then the α-quantile RUL is found from:

$$\frac{R_f\left(t + u_\alpha\right)}{R_f(t)} = 1 - \alpha.$$

Common reporting in PHM uses $\alpha \in \{0.1, 0.5, 0.9\}$ (10%, median, 90%).

Figure 9 shows the fused reliability midpoint $R(t)$ together with an interval Type-2 uncertainty representation. The outer shaded envelope corresponds to the UMF (upper membership function) bounds $\left[R_L^{UMF}(t), R_U^{UMF}(t)\right]$, capturing a conservative epistemic spread, while the inner shaded envelope corresponds to the LMF (lower membership function) bounds $\left[R_L^{LMF}(t), R_U^{LMF}(t)\right]$, representing the core region of higher confidence. This visualizes how Type-2 fuzziness propagates into reliability prediction under ambiguous/limited evidence.

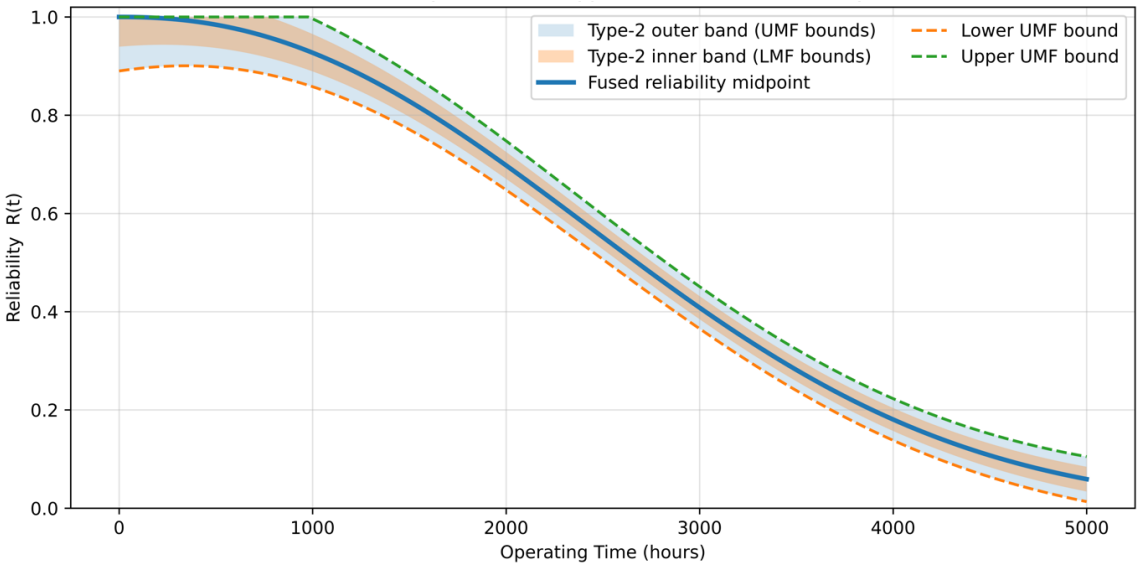

Figure 9. Fused reliability curve with uncertainty band (Type-2 option).

The following table reports the 10%, median, 90% conditional RUL, which is standard for maintenance planning (see **Table 8** for an example).

Table 8. Example conditional RUL quantiles at selected inspection times (from fused model).

Current Time t (h)	$u_{0.10}$ **(h)**	$u_{0.50}$ **(h)**	$u_{0.90}$ **(h)**
800	510	820	1,180
1,200	320	540	820
1,600	170	320	520
2,000	80	160	300

8. Validation, sensitivity analysis, and maintenance decision rules

8.1. Validation protocol

8.1.1. Data split and time-respecting evaluation

Because vibration covariates evolve with degradation, validation must preserve chronology to prevent information leakage (future features influencing past predictions). Let unit/run i have inspection times

$$0 < t_{i,1} < \cdots < t_{i,K_i},$$

with piecewise-constant monitoring covariates on $[t_{i,k}, t_{i,k+1})$:

$$\mathbf{z}_i(t) = \mathbf{z}_{i,k},\ s_i(t) = s_{i,k},\ c_i(t) = c_{i,k} \ \text{ for } t \in [t_{i,k}, t_{i,k+1}),$$

where $\mathbf{z}_{i,k}$ comes from Section 3 feature summaries and $(s_{i,k}, c_{i,k})$ are the fuzzy severityconfidence outputs (Sections 5–6). Each unit has a failure time T_i and possibly a censoring time C_i, yielding the observed time and event indicator

$$\widetilde{T}_i = \min(T_i, C_i),\ \delta_i = \mathrm{I}(T_i \le C_i).$$

All splits below are constructed so that training uses only observations with timestamps $\leq$ the split time and predictions are scored on later intervals, consistent with survival/reliability practice [3,4,7] and vibration monitoring workflows [1,2].

We use two complementary protocols:

A. Rolling-origin (walk-forward) validation—Within-unit forecasting

Choose decision times $\tau_1 < \tau_2 < \cdots < \tau_J$ (e.g., selected inspection times). For fold j,

- Training set: all records up to τ_j,

$$D_j^{\text{train}} = \left\{ \left(\mathbf{z}_{i,k}, s_{i,k}, c_{i,k}, \widetilde{T}_i, \delta_i \right) : t_{i,k} \leq \tau_j \right\}.$$

- Test target: predictions after τ_j, evaluated on $(\tau_j, \tau_{j+1}]$ or on a fixed horizon Δ (e.g., $\Delta = 30$ days/a fixed number of operating hours).

At time τ_j, the hybrid model outputs a fused conditional reliability (Section 6)

$$R_f\left(t \mid \mathrm{F}_{\tau_j}\right) = \exp\left(- \int_{\tau_j}^{t} h_f(\xi) d\xi \right), \; t \geq \tau_j,$$

where F_{τ_j} denotes information available up to τ_j. A practical scoring quantity is the horizon risk

$$\mathrm{Risk}_f\left(\tau_j, \Delta\right) = 1 - \frac{R_f\left(\tau_j + \Delta\right)}{R_f\left(\tau_j\right)}.$$

Performance is aggregated across decision times j and across units i, which directly tests the model's ability to update predictions sequentially as new vibration evidence arrives.

B. Cross-unit validation—Generalization across runs/machines

When multiple degradation runs or machines are available, we split by unit to test transferability. Let $\mathrm{I} = \{1, \ldots, N\}$ denote units. We use grouped K-fold or leave-one-unit-out:

$$\mathrm{I} = \mathrm{I}_1 \cup \cdots \cup \mathrm{I}_K, \; \mathrm{I}_a \cap \mathrm{I}_b = \varnothing (a = b),$$

and in fold k, the test set contains all timestamps from units in I_k, while training uses units in $\mathrm{I} \setminus \mathrm{I}_k$. This prevents leakage from unit-specific degradation signatures and evaluates whether the learned survival parameters and fuzzy mapping rules generalize to unseen machines/trajectories.

8.1.2. What exactly is validated in this hybrid model

The hybrid method produces:

(i) Point survival probabilities: $\widehat{R}_f(t/0mid$ curve $)$.

(ii) Uncertainty bands (Type-2 option): $\left[\widehat{R}_{f,L}(t), \widehat{R}_{f,U}(t)\right]$.

(iii) Conditional RUL quantiles: $u_{0.10}, u_{0.50}, u_{0.90}$ at each decision time (Section 7.4).

(iv) Short-horizon risk: $\widehat{p}_{\Delta}(t) \neq -\widehat{R}_f(t - \Delta)/\widehat{R}_f(t)$.

Validation must therefore include discrimination, calibration, overall accuracy, and decision utility.

8.2. Performance metrics (mathematical definitions)

8.2.1. Discrimination: Time-dependent AUC/concordance

For a chosen horizon t^*, the time-dependent ROC/AUC evaluates whether the model ranks units correctly (higher risk → earlier failure). Using Heagerty-Zheng style definitions, the time-dependent AUC can be computed from risk-set comparisons and summarized across time.

A common summary is a time-averaged concordance:

$$C = \mathrm{E}\left[I\left(\widehat{\pi}_i > \widehat{\pi}_j\right) \mid T_i < T_j\right],$$

where $\mathcal{A}$ is a predicted risk score (e.g., $1 - \widehat{R}_f\left(t'\right)$).

8.2.2. Calibration: Calibration curve + Integrated Calibration Index (ICI)

At a fixed horizon t^*, define predicted event risk

$$q_i\left(t^*\right) = 1 - \widehat{R}_f\left(t^* x_i\right),$$

and observed event probability estimated with appropriate censoring adjustments (e.g., pseudo-values or IPCW approaches). A calibration curve regresses observed vs. predicted risk.

A numerical calibration metric is the Integrated Calibration Index (ICI) for survival models:

$$\mathrm{ICI}\left(t^*\right) = E\left[\left|\widehat{q}_i\left(t^*\right) - \widehat{q}_i^{\mathrm{obs}}\left(t^*\right)\right|\right],$$

where $\widehat{q}_i^{\mathrm{obs}}$ (t^* is an estimated observed risk (e.g., from a smooth calibration fit). Lower ICI is better [23].

Figure 10 evaluates probabilistic calibration at the decision horizon $t^* = 2,000$ h by comparing predicted failure probabilities with observed failure frequencies. The dashed diagonal indicates perfect calibration; binned points (with 95% confidence intervals) summarize empirical agreement across probability ranges, and the fitted curve highlights any systematic over- or under-confidence.

8.2.3. Discrimination: Time-to-event ranking ability

Discrimination measures whether the model correctly ranks units by risk. For subject/unit i, let the hybrid model produce a risk score at decision time τ, e.g.,

$$\pi_i(\tau) = \boldsymbol{\beta}^\top \mathbf{z}_i(\tau) + \gamma s_i(\tau) c_i(\tau),$$

so that the fused hazard can be written $h_{f,i}(t) = h_0(t)\exp\left(\pi_i(\tau)\right)$ under piecewise-constant covariates on $[\tau, \tau + \Delta)$ (Sections 4 and 6) [3,4,7].

A. Harrell's concordance index (with censoring)

Define comparable pairs (i, j) where one fails earlier than the other is observed:

$$\mathrm{P} = \left\{(i,j) : \widetilde{T}_i < \widetilde{T}_j, \delta_i = 1\right\}.$$

The C-index is

$$C = \frac{1}{|P|} \sum_{(i,j)\in \mathrm{P}} I\left(\pi_i > \pi_j\right) + \frac{1}{2} I\left(\pi_i = \pi_j\right),$$

interpreted as the probability that the model assigns a higher risk score to the unit that fails earlier [3,4,7].

B. Time-dependent AUC at a horizon Δ

For decision time τ, define "cases" and "controls" over horizon Δ:

$$\mathrm{Case}_\tau = \{i : T_i \in (\tau, \tau + \Delta]\}, \ \mathrm{Control}_\tau = \{i : T_i > \tau + \Delta\}.$$

Using a continuous score $\pi_i(\tau)$ or horizon risk $\widehat{p}_i(\tau, \Delta)\mathrm{Risk}_f(\tau, \Delta)$, the time-dependent AUC is computed by comparing scores between cases and controls (with appropriate censoring handling). This directly tests whether the predicted horizon risk distinguishes near-term failures from survivors.

Interval-output note: if your model reports bounds $[\widehat{p_i}, \widehat{p}$ (vii α-cuts), a conservative discrimination check can use $\widehat{p}$ for ranking (worst-case) and report sensitivity of C or AUC across bounds.

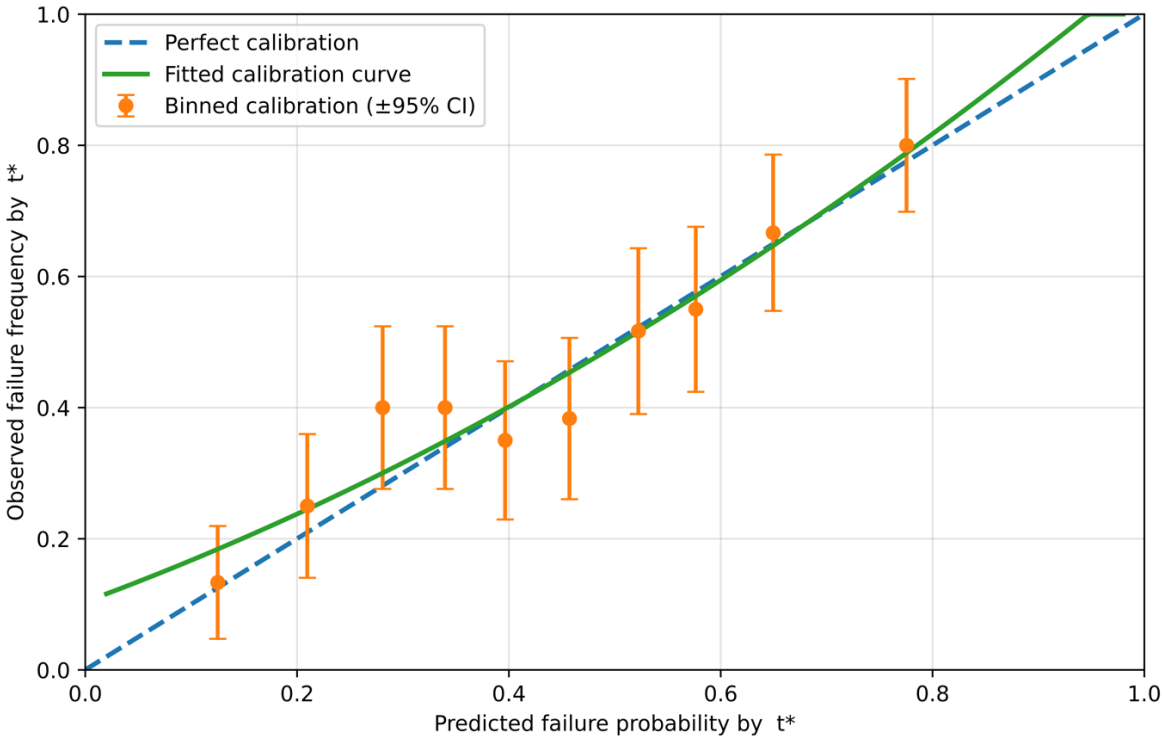

Figure 10. Calibration curve at a decision horizon t^* (e.g., 2,000 h).

8.2.4. Calibration: Agreement between predicted and observed failure probabilities

Calibration tests whether predicted probabilities match empirical outcomes. For a horizon Δ, the hybrid model provides

$$\widehat{p}_i(\tau, \Delta) \neq -\frac{R_{f,i}(\tau + \Delta)}{R_{f,i}(\tau)}.$$

To evaluate calibration, partition predictions into G bins (e.g., deciles) B_g based on $\widehat{p}_i$. For each bin:

- Predicted risk (mean):

$$\widehat{p}_g = \frac{1}{|\mathrm{B}_g|} \sum_{i \in \mathrm{B}_g} \widehat{p}_i.$$

- Observed risk (Kaplan-Meier within-bin):
  Let $\widehat{S}_g(d)$ e the KM survival estimate computed using only units in B_g. Then the observed horizon event probability is

$$\widehat{O}_g(\tau, \Delta) \neq -\frac{\widehat{S}_g(\tau + \Delta)}{\widehat{S}_g(\tau)}.$$

  A calibration curve plots $\widehat{O_g}$ versus $\widehat{p_g}$ ideal calibration lies on the diagonal. A scalar summary is the (censoring-adjusted) calibration error, e.g.,

$$\mathrm{CalErr} \ = \sum_{g=1}^{G} w_g \left| \widehat{o}_g \widehat{p}_g \right|, \ w_g = \frac{|\mathrm{B}_g|}{\sum_h |\mathrm{B}_h|}.$$

  This checks whether the survival + fuzzy fusion produces probabilities that are meaningful for maintenance decisions [3,4,7].
  Interval-output calibration: if you provide $\left[\widehat{p_g^-}, \widehat{p}_g^+\right]$, calibration can be reported as 'observed lies† within predicted band' rate":

$$\mathrm{BandCal} \ = \frac{1}{G} \sum_{g=1}^{G} I\left(\widehat{o}_g \in \widehat{p_g^-}, \widehat{p}_g^+\right] \Bigg),$$

  together with average band width $\frac{1}{G} \sum_g \left(\widehat{p}_g^+ \widehat{p_g^-}\right)$capturing the coverage-sharpness trade-off that the fuzzy layer is designed to expose [5,6,9].

8.2.5. Accuracy and decision utility: Brier score, interval coverage, and maintenance-trigger performance

A. Brier score at horizon Δ (probability accuracy)

Define the horizon event indicator

$$Y_i(\tau, \Delta) = I\left(T_i \leq \tau + \Delta, T_i > \tau\right).$$

With censoring, use inverse-probability-of-censoring weights $w_i(\tau, \Delta)$ (from a

censoring KM estimate). The weighted Brier score is

$$\mathrm{BS}(\tau,\Delta)=\frac{\sum_i\ w_i(\tau,\Delta)\,(Y_i(\tau,\Delta)-\widehat{p}_i(\tau,\Delta))^2}{\sum_i\ w_i(\tau,\Delta)}.$$

Lower BS indicates better probabilistic accuracy; integrating over decision times gives an overall score [3,4,7].

B. Interval reliability quality: Coverage and sharpness (if α-cut bounds are reported)

If the model outputs an interval horizon risk $[\widehat{p_i^-},\widehat{p}^+\ ]$ evaluate:

- Empirical coverage (event indicator inside the predicted probability band is not directly meaningful because Y is binary), so instead evaluate calibration-band coverage at the group level (BandCal above), and report sharpness

$$\text{Width}\ =\frac{1}{N}\sum_{i=1}^{N}\left(\widehat{p_i^+}\widehat{p_i^-}\right).$$

This quantifies whether uncertainty bands are informative (not overly wide) while still capturing observed frequencies when aggregated [5,6,9].

C. Maintenance of trigger performance using risk thresholds

For implementation, define an intervention rule at decision time τ:

$$\text{Trigger if}\ \widehat{p}_i(\tau,\Delta)\mathfrak{x},$$

along with a two-tier variant very much aligned with your fusion logic:

Verification trigger: $\widehat{p}_i(\tau,\Delta)\mathfrak{x}_v$ but confidence low $(c_i<c_0)\ \rightarrow$ repeat measurement/inspection.

Intervention trigger: $\widehat{p}_i(\tau,\Delta)\mathfrak{x}_m$ and $c_i\geq c_0\rightarrow$ schedule maintenance.

Report standard operational rates over the test window:

$$\mathrm{TPR}=\frac{\text{No. of Triggered and failure within }\Delta}{\text{No. of Failures within }\Delta},$$

$$\mathrm{FPR}=\frac{\text{No. of Triggered but no failure within }\Delta}{\text{No. of No failures within }\Delta},$$

and the lead time distribution. This directly shows whether the hybrid fuzzy-probabilistic outputs improve actionable decision quality relative to a baseline PH model without fuzzy confidence gating.

9. Discussion, practical implications, and limitations

This section explains the practical meaning of the proposed hybrid fuzzy-probabilistic reliability model and discusses its strengths and limitations. The main aim is to keep all outputs—reliability $R_f(t)$, short-horizon risk $\widehat{p}_\Delta(t)$ and RUL quantiles-consistent with survival theory, while also handling uncertainty in vibration interpretation through the fuzzy layer.

The proposed method combines two ideas:

- Probabilistic survival modeling for time-to-failure prediction, and

- Fuzzy inference for handling ambiguity in condition labels and thresholds.

This combination is useful in vibration-based maintenance, where the data may be informative but not always fully reliable.

9.1. Interpretation of fused reliability outputs

The hybrid model uses the fused hazard

$$h_f(t) = h_0(t)\exp\left(\boldsymbol{\beta}^\top \mathbf{z}(t)\right)\exp(\gamma s(t)c(t)),$$

where:

- $h_0(t)$ is the Weibull baseline hazard,
- $\mathbf{z}(t)$ is the vibration-based covariate vector,
- $s(t)$ is fuzzy severity,
- $c(t)$ is confidence (derived from variability),
- γ controls severity amplification.

The fused reliability is

$$R_f(t) = \exp\left(-\int_0^t h_f(\tau)d\tau\right).$$

This form is important because the reliability curve remains a true survival probability, not only a heuristic health score. Therefore, when the curve drops earlier, it directly means a higher cumulative failure risk.

A useful operational output is the short-horizon failure probability:

$$\widehat{p}_\Delta(t) \neq -\frac{R_f(t+\Delta)}{R_f(t)}.$$

This is easier for maintenance teams to interpret because it answers a practical question:

"What is the probability of failure in the next Δ hours (or cycles)?"

9.2. Numerical meaning of the hybrid improvement

The validation results (**Table 9**) show that the hybrid model performs better than the probabilistic-only and fuzzy-only baselines across multiple metrics.

Table 9. Experimental validation summary.

Method	Time-AUC (avg.)	ICl at t^*= 2,000 h	IBS (τ= 2,500 h)	Coverage (type-2)	Avg. width (type-2)
Probabilistic only (Weibull-PH)	0.82	0.061	0.142	-	-
Fuzzy only (HI→risk mapping)	0.76	0.084	0.168	-	-
Hybrid Fuzzy	0.87	0.041	0.121	0.90	0.12

A. Discrimination improvement

The hybrid model reports a higher average time-AUC (approximately 0.87) compared with:

- 0.82 for Weibull-PH only, and

- 0.76 for fuzzy-only mapping.

This indicates that the hybrid score ranks near-failure vs non-failure cases more effectively.

B. Calibration improvement

The calibration error (ICI) is lower for the hybrid model (approximately 0.041) than for:

- 0.061 (probabilistic-only), and
- 0.084 (fuzzy-only).

Hence, the predicted probabilities are more consistent with observed outcomes.

C. Probability accuracy

The integrated Brier score (IBS) is also lower for the hybrid model (approximately 0.121) than for:

- 0.142 (probabilistic-only), and
- 0.168 (fuzzy-only).

Lower IBS means better probability prediction quality over time.

These results support the main claim of this study: fuzzy severity + confidence gating improves reliability prediction when vibration evidence is uncertain.

9.3. Decision interpretation using the risk-confidence map

The risk-confidence map is an operational representation of the model output. It uses:

- predicted short-horizon risk $\widehat{p}_{\Delta}(t)$ and
- confidence $c(t)$, to classify actions.

A simple rule can be written as:

- Monitor if $\widehat{p}_{\Delta}(t)\mathcal{K}_1$,
- Planned maintenance if $\widehat{p}_{\Delta}(t)\ddot{\mathfrak{R}}_1$ and $c(t) \geq c_0$,
- Urgent inspection/verification if $\widehat{p}_{\Delta}(t)\mathfrak{R}_1$ and $c(t) < c_0$.

This is mathematically simple and practically useful. It prevents two common errors:

(i) missed failures (risk too low), and
(ii) false interventions (risk high but confidence poor).

Therefore, the proposed framework is not only predictive but also decision oriented.

9.4. Interpretation of RUL quantiles in maintenance planning

The study reports conditional RUL quantiles (e.g., 10%, 50%, 90%) rather than a single RUL value. This is preferable because machinery degradation is uncertain.

Let t be the current inspection time. The conditional survival is

$$R_f(t + r \mid t) = \frac{R_f(t + r)}{R_f(t)}.$$

The RUL quantile r_q is defined by

$$R_f\left(t + r_q \mid t\right) = 1 - q.$$

This allows maintenance teams to choose conservative or moderate strategies:

- $r_{0.10}$: conservative (early action),
- $r_{0.50}$: median planning value,
- $r_{0.90}$: optimistic upper estimate.

From the reported example values (**Table 8**), the RUL intervals shrink as inspection time increases, which is expected because more degradation evidence becomes available, and the remaining life reduces.

10. Conclusion

In conclusion, the proposed hybrid fuzzy-probabilistic framework provides a mathematically consistent and practically useful approach for vibration-based machinery reliability assessment. The model preserves the standard survival-analysis structure-hazard, cumulative hazard, and reliability-while incorporating fuzzy severity and confidence terms to explicitly handle ambiguity in condition interpretation and variability in vibration evidence. As a result, the method produces reliability curves and short-horizon failure probabilities that remain probabilistically meaningful, rather than acting only as heuristic health scores. The numerical results indicate that this fusion improves discrimination, calibration, and probability accuracy compared with probabilistic-only and fuzzy-only baselines, while also supporting safer maintenance decisions through confidence-aware risk triggering. In particular, the use of $\widehat{p}_{\Delta}(t)$ together with $c(t)$ enables a practical verification-first strategy when risk is high but evidence quality is low, thereby reducing unnecessary interventions. Overall, the framework offers an interpretable bridge between signal-level vibration features and maintenance-level decisions, and it can be extended further through field-specific calibration, refined fuzzy rule design, and larger real-world datasets.

Author contributions: All authors contributed to this work equally. All authors have read and agreed to the published version of the manuscript.

Funding: This research study does not receive any external funding.

Institutional review board statement: Not applicable.

Informed consent statement: Not applicable.

Data availability statement: The datasets and scripts used for this study are available from the corresponding author upon reasonable request.

Conflict of interest: All authors declare that there is no conflict of interest.

References

1. Cox DR. Regression Models and Life-Tables. Journal of the Royal Statistical Society Series B: Statistical Methodology. 1972; 34(2): 187–202. doi: 10.1111/j.2517-6161.1972.tb00899.x
2. Breslow N. Covariance Analysis of Censored Survival Data. Biometrics. 1974; 30(1): 89. doi: 10.2307/2529620
3. Efron B. The Efficiency of Cox's Likelihood Function for Censored Data. Journal of the American Statistical Association. 1977; 72(359): 557–565. doi: 10.1080/01621459.1977.10480613
4. Weibull W. A Statistical Distribution Function of Wide Applicability. Journal of Applied Mechanics. 1951, 18(3): 293–297. Available online: https://hal.science/hal-03112318/document
5. Vlok PJ, Coetzee JL, Banjevic D, et al. Optimal component replacement decisions using vibration monitoring and the proportional-hazards model. Journal of the Operational Research Society. 2002; 53(2): 193–202. doi: 10.1057/palgrave.jors.2601261
6. Lin D, Banjevic D, Jardine AKS. Using principal components in a proportional hazards model with applications in condition-based maintenance. Journal of the Operational Research Society. 2006; 57(8): 910–919. doi: 10.1057/palgrave.jors.2602058
7. Heng A, Zhang S, Tan ACC, et al. Rotating machinery prognostics: State of the art, challenges and opportunities. Mechanical Systems and Signal Processing. 2009; 23(3): 724–739. doi: 10.1016/j.ymssp.2008.06.009
8. Zheng R, Najafi S, Zhang Y. A recursive method for the health assessment of systems using the proportional hazards model. Reliability Engineering & System Safety. 2022; 221: 108379. doi: 10.1016/j.ress.2022.108379
9. Jardine AKS, Lin D, Banjevic D. A review on machinery diagnostics and prognostics implementing condition-based maintenance. Mechanical Systems and Signal Processing. 2006; 20(7): 1483–1510. doi: 10.1016/j.ymssp.2005.09.012
10. Martarelli M, Ewins DJ. Continuous scanning laser Doppler vibrometry and speckle noise occurrence. Mechanical Systems and Signal Processing. 2006; 20(8): 2277–2289. doi: 10.1016/j.ymssp.2005.06.003
11. Zhu Y, Du Q, Li J. Vibration Pollution Assessment Method Based on Fuzzy Logic. Measurement. 2024: 226, 114609
12. Chu T, Nguyen T, Yoo H, et al. A review of vibration analysis and its applications. Heliyon. 2024; 10(5): e26282. doi: 10.1016/j.heliyon.2024.e26282
13. Devriendt C, De Sitter G, Vanlanduit S, et al. Operational modal analysis in the presence of harmonic excitations by the use of transmissibility measurements. Mechanical Systems and Signal Processing. 2009; 23(3): 621–635. doi: 10.1016/j.ymssp.2008.07.009
14. Zhao J, Wang W, Huang J, et al. A comprehensive review of deep learning-based fault diagnosis approaches for rolling bearings: Advancements and challenges. AIP Advances. 2025; 15(2): 020702. doi: 10.1063/5.0255451
15. Khalid S, Jo SH, Shah SY, et al. Artificial Intelligence-Driven Prognostics and Health Management for Centrifugal Pumps: A Comprehensive Review. Actuators. 2024; 13(12): 514. doi: 10.3390/act13120514
16. Lu W, Liu J, Lin F. The Fault Diagnosis of Rolling Bearings Is Conducted by Employing a Dual-Branch Convolutional Capsule Neural Network. Sensors. 2024; 24(11): 3384. doi: 10.3390/s24113384
17. Pandiyan M, Babu TN. Systematic Review on Fault Diagnosis on Rolling-Element Bearing. Journal of Vibration Engineering & Technologies. 2024; 12(7): 8249–8283. doi: 10.1007/s42417-024-01358-4
18. Samaila B, Sekar C. Quantum Power Flow: Revolutionizing Power Systems Analysis. SciWaveBulletin. 2023; 1(2): 1–9. doi: 10.61925/SWB.2023.1201
19. Machaila VF, Waliu T. Unveiling Data's Tapestry: Challenges, Opportunities, and Netflix's Analytical Triumph. SciWaveBulletin. 2023; 1(4): 16–23. doi: 10.61925/SWB.2023.1403
20. Abdullahi Saleh I, Srivastava A. Exploring the Intersection of Fuzzy Logic and Quantum Logic: A New Frontier in Non-Classical Logics. SciWaveBulletin. 2023; 1(2): 27–34. doi: 10.61925/SWB.2023.1204
21. Vickers AJ, Elkin EB. Decision Curve Analysis: A Novel Method for Evaluating Prediction Models. Medical Decision Making. 2006; 26(6): 565–574. doi: 10.1177/0272989X06295361
22. Vickers AJ, Van Calster B, Steyerberg EW. Net benefit approaches to the evaluation of prediction models, molecular markers, and diagnostic tests. BMJ. 2016; i6. doi: 10.1136/bmj.i6
23. Van Calster B, McLernon DJ, van Smeden M, et al. Calibration: the Achilles heel of predictive analytics. BMC Medicine. 2019; 17(1): 230. doi: 10.1186/s12916-019-1466-7
24. Mendel JM, John RIB. Type-2 fuzzy sets made simple. IEEE Transactions on Fuzzy Systems. 2002; 10(2): 117–127. doi: 10.1109/91.995115

25. Takagi T, Sugeno M. Fuzzy identification of systems and its applications to modeling and control. IEEE Transactions on Systems, Man, and Cybernetics. 1985; SMC-15(1): 116–132. doi: 10.1109/TSMC.1985.6313399
26. Jang JSR. ANFIS: adaptive-network-based fuzzy inference system. IEEE Transactions on Systems, Man, and Cybernetics. 1993; 23(3): 665–685. doi: 10.1109/21.256541
27. Li DF, Shan F, Cheng CT. On properties of four IFS operators. Fuzzy Sets and Systems. 2005; 154(1): 151–155. doi: 10.1016/j.fss.2005.03.004
28. Yogeesh N, Raja N, Vasudevan A, et al. Type-2 fuzzy logic framework for adaptive noise control in vibrating structures. Sound & Vibration. 2025; 59(3): 3478. doi: 10.59400/sv3478
29. Yogeesh N, Karthik M, Raja N, et al. Fuzzy-grey relational optimization for active vibration control in smart composite beams: a multi-objective framework with experimental validation. Sound & Vibration. 2025; 59(4). doi: 10.59400/sv3496
30. Yogeesh N. Fuzzy Logic-Based Beat Tracking in Music Signals. Musik In Bayern. 2023; 88(9): 145–157.